Extended Higgs Sectors as Windows into Dark Matter: Probing New Physics at Colliders

Juhi Dutta

From Big Bang to Now: A Theory-Experiment Dialogue
SRM, AP

The Institute of Mathematical Sciences, India

based on *Eur.Phys.J.C 84(2024) 9,926* with J.Lahiri, C.Li, G. Moortgat-Pick, S.F. Tabira, J.A.Ziegler

January 23-25, 2025

The Standard Model of Particle Physics

- The Standard Model of Particle Physics is a quantum field-theoretic framework describing all matter content of the Universe and three of the four forces, including electromagnetism, weak and strong force.

- The SM is a gauge theory where the underlying symmetry is $SU(3)_C$X $SU(2)_L$ X $U(1)_Y$ corresponding to colour, weak isospin and hypercharge respectively.

Particle content

- Matter content of SM: six quarks, three charged leptons, three massless neutrinos and a scalar Higgs boson.
- Force mediators: eight gluons, photon, $W^{\pm}$ and Z mediating strong force, electromagnetic force and weak force respectively.

Name	$SU(3)_C$	$SU(2)_L$	$U(1)_Y$
$q_L^i = \begin{pmatrix} u_L^i \\ d_L^i \end{pmatrix}$	3	2	1/3
u_R^i	3	1	4/3
d_R^i	3	1	-2/3
$\ell_L^i = \begin{pmatrix} \nu_L^i \\ e_L^i \end{pmatrix}$	1	2	-1
e_R^i	1	1	-2
$\phi = \begin{pmatrix} \phi^+ \\ \phi^0 \end{pmatrix}$	1	2	1
G_μ	8	1	0
W_μ	1	3	0
B_μ	1	1	0

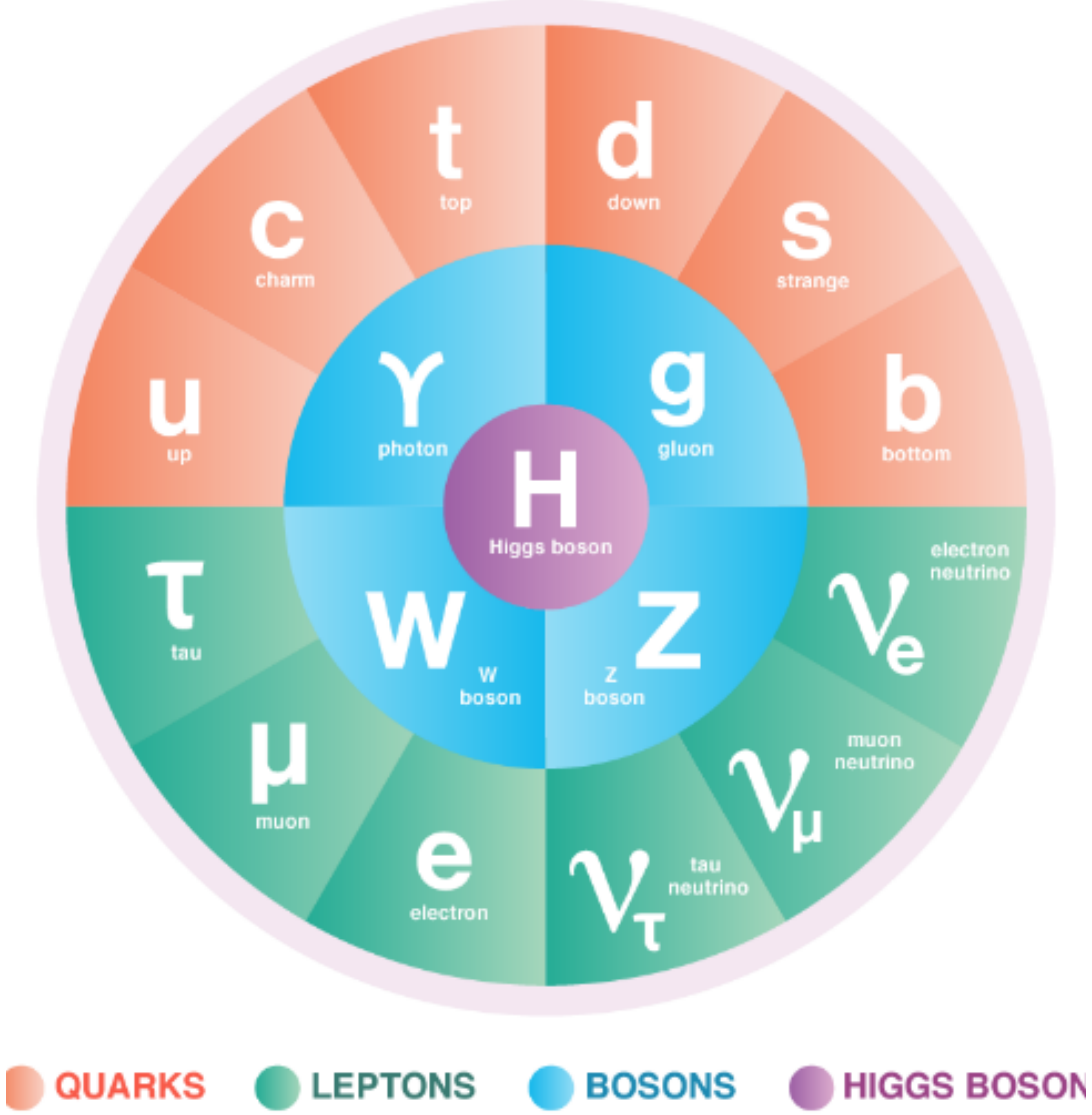

The Standard Model of Particle Physics, FERMILAB

Why New Physics?

- Gauge hierarchy problem
- Dark Matter
- Dark Energy
- Non-zero neutrino masses
- Matter-antimatter asymmetry
- Strong CP-problem
- Gravity

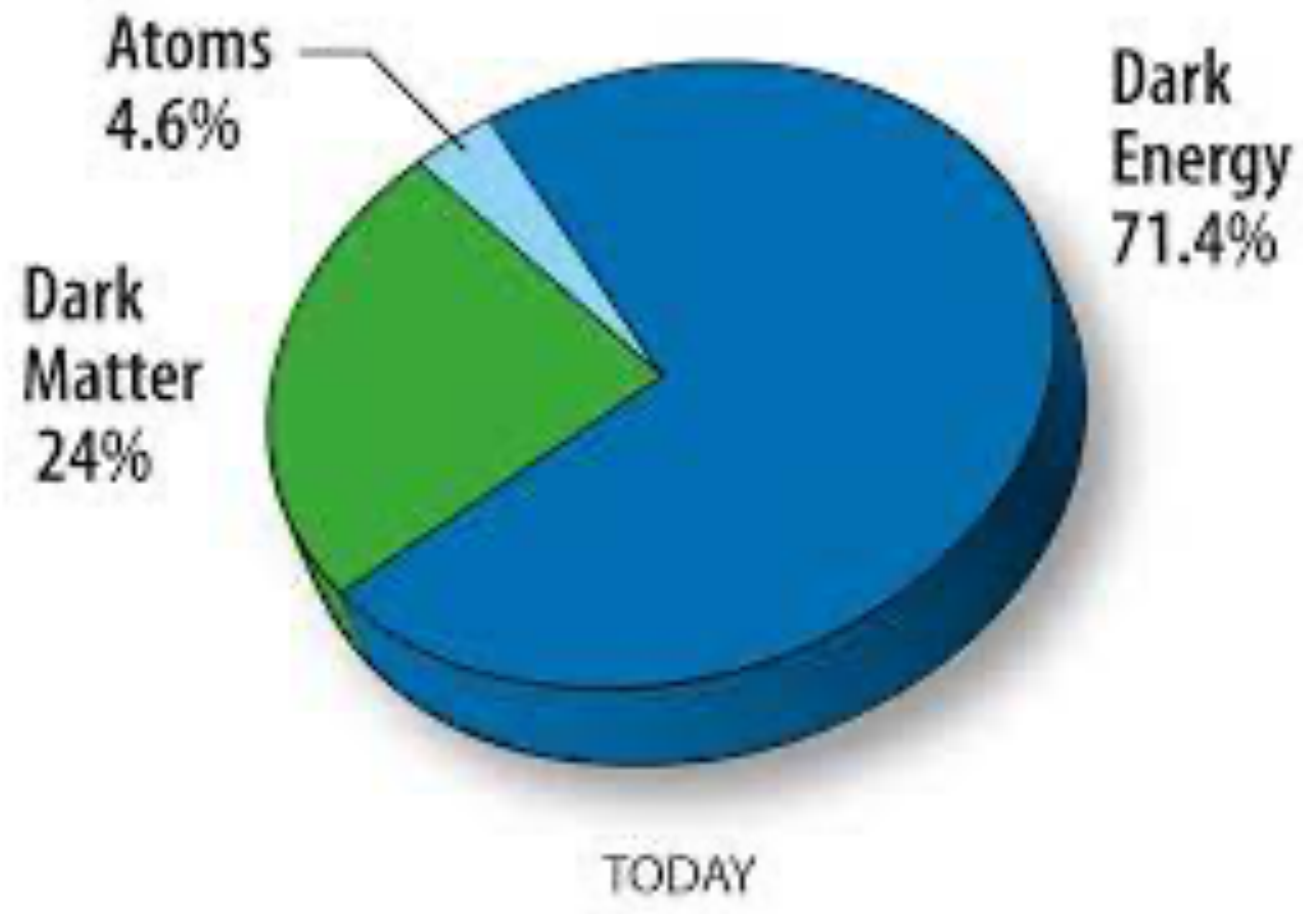

NASA.

Extended Higgs Sectors: 2HDMS

Interplay of Dark Matter and Higgs Phenomenology

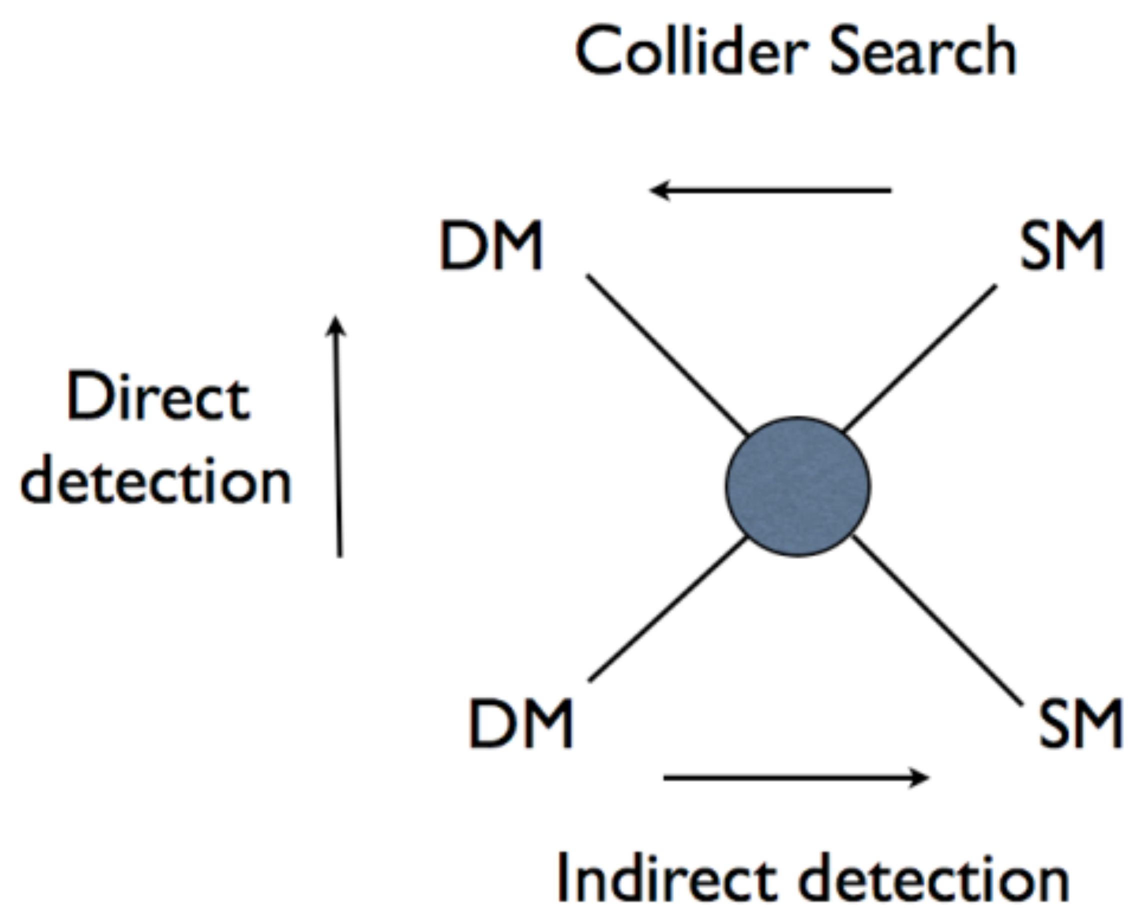

Motivation

- Scalar singlets under the SM gauge group $\Longrightarrow$ potential dark matter candidates

- Communicates to the SM via the 125 GeV Higgs as the portal to the dark sector, however stringently constrained from dark matter direct detection data.

Barger, et.al Phys.Rev.D79:015018,2009

- Presence of additional portals to dark matter via extra Higgses as in singlet extended multi-Higgs models (N2HDM) relaxes direct detection constraints with prospects for collider signals.

Drozd et.al JHEP11 (2014) 105, Dey et.al JHEP 09 (2019) 004

- Scalar extensions with real/complex scalar singlets in the context of 2HDM also address baryogenesis, inflation and strong CP-problem.

Dutta et.al, 2309.10857

- Presence of a complex singlet provides an extra degree of freedom to address recent excesses observed at the LHC in conjunction with dark matter.

The Model

- Consider a softly broken Z_2 (to avoid FCNC) symmetric Type II 2HDM augmented with a complex scalar singlet S, stabilized under Z_2'.

- SM quantum numbers:

Fields	Z_2	Z_2'
Φ_1	+1	+1
Φ_2	-1	+1
S	+1	-1

$$\Phi_i = \begin{pmatrix} \phi_i^{\pm} \\ \frac{1}{\sqrt{2}}(v_i + h_i + i a_i) \end{pmatrix}, \quad i = 1, 2,$$

$$S = \frac{1}{\sqrt{2}}(v_S + h_S + i a_S)$$

- The scalar potential is: $V_{2HDMS} = V_{2HDM} + V_S,$

$$V_{2HDM} = m_{11}^2 \Phi_1^\dagger \Phi_1 + m_{11}^2 \Phi_1^\dagger \Phi_1 - (m_{12}^2 \Phi_1^\dagger \Phi_2 + h.c) + \frac{\lambda_1}{2}(\Phi_1^\dagger \Phi_1)^2 + \frac{\lambda_2}{2}(\Phi_2^\dagger \Phi_2)^2 + \lambda_3(\Phi_1^\dagger \Phi_1)(\Phi_2^\dagger \Phi_2) + \frac{\lambda_4}{2}(\Phi_1^\dagger \Phi_2)(\Phi_2^\dagger \Phi_1) + \frac{\lambda_5}{2}(\Phi_1^\dagger \Phi_2)^2 + h.c,$$

$$V_S = m_S^2(S^\dagger S) + \frac{m_S^{2'}}{2}(S^2 + h.c) + \frac{\lambda_1''}{24}(S^4 + h.c) + \frac{\lambda_2''}{6}(S^2(S^\dagger S) + h.c) + \frac{\lambda_3''}{4}(S^\dagger S)^4 +$$

$$\lambda_1' S^\dagger S \Phi_1^\dagger \Phi_1 + \lambda_2' S^\dagger S \Phi_2^\dagger \Phi_2 + S^2(\lambda_4' \Phi_1^\dagger \Phi_1 + \lambda_5' \Phi_2^\dagger \Phi_2) + h.c.$$

Baum, et.al, *JHEP*12(2018)044

- After electroweak symmetry breaking, particle content: $h_1, h_2, h_3, A, H^{\pm}, A_S$.

- The lightest Higgs h_1 = 95 GeV, and h_2 ~ 125 GeV.

- Work in the mass basis: $m_{h_1}, m_{h_2}, m_{h_3}, m_A, m_{H^{\pm}}, \tan\beta, \tilde{\mu}^2, c_{h_1bb}, c_{h1tt}, alignm,$
$m_{A_S}, v_S, \delta'_{14}(= \lambda'_4 - \lambda'_1), \delta'_{25}(= \lambda'_5 - \lambda'_2), m_S^{2'},$

where $\tan\beta = \frac{v_2}{v_1}, alignm = |\sin(\beta - (\alpha_1 + \alpha_3 \cdot \mathrm{sgn}(\alpha_2)))| \approx 1, \tilde{\mu}^2 = \frac{m_{12}^2}{\sin\beta\cos\beta}.$

- Couplings of the 95 GeV higgs:

$$c_{h_1 t\bar{t}} = \frac{R_{12}}{\sin\beta}, \qquad \mu_{b\bar{b}}^{2HDMS} \propto |c_{h_1VV}|^2,$$

$$c_{h_1 b\bar{b}} = \frac{R_{11}}{\cos\beta}, \qquad \mu_{\gamma\gamma}^{2HDMS} \propto \frac{(|c_{h_1t\bar{t}}|)^2}{(|c_{h_1b\bar{b}}|)^2} \propto (\frac{\tan\alpha_1}{\tan\beta})^2$$

$$c_{h_1\tau\tau} = \frac{R_{11}}{\cos\beta},$$

$$R = \begin{pmatrix} c_{\alpha_1}c_{\alpha_2} & s_{\alpha_1}c_{\alpha_2} & s_{\alpha_2} \\ -s_{\alpha_1}c_{\alpha_3} - c_{\alpha_1}s_{\alpha_2}s_{\alpha_3} & c_{\alpha_1}c_{\alpha_3} - s_{\alpha_1}s_{\alpha_2}s_{\alpha_3} & c_{\alpha_2}s_{\alpha_3} \\ s_{\alpha_1}s_{\alpha_3} - c_{\alpha_1}s_{\alpha_2}c_{\alpha_3} & -c_{\alpha_1}s_{\alpha_3} - s_{\alpha_1}s_{\alpha_2}c_{\alpha_3} & c_{\alpha_2}c_{\alpha_3} \end{pmatrix}$$

$$c_{h_1VV} = \cos\beta R_{11} + \sin\beta R_{12},$$

S.Heinemeyer et.al,
Phys. Rev. D 106 (2022), no. 7 075003
(2HDMS-Z_3 symmetric case)

Dark Sector

- Mass: $m_{A_S}^2 = -(2m_S'^2 + \frac{2\lambda_1''}{3}v_S^2 + 2(\lambda_4' v_1^2 + \lambda_5' v_2^2))$

- Trilinear couplings:

$$\begin{aligned}
\frac{\lambda_{h_j A_S A_S}}{v} = &[\frac{\sum_{i=1}^{3} m_{h_i}^2 R_{i1}R_{i3}}{3vv_S\cos(\beta)} + \frac{4\delta_{14}'}{3}]c_\beta R_{j1} \\
&+ [\frac{\sum_{i=1}^{3} m_{h_i}^2 R_{i2}R_{i3}}{3vv_S\sin(\beta)} + \frac{4\delta_{25}'}{3}]s_\beta R_{j2} \\
&- [\frac{2}{vv_S}(2m_S'^2 + m_{A_S}^2 + (\frac{\sum_{i=1}^{3} m_{h_i}^2 R_{i1}R_{i3}}{3vv_S\cos(\beta)} + \frac{\delta_{14}'}{3})2v^2c_\beta^2 \\
&+ (\frac{\sum_{i=1}^{3} m_{h_i}^2 R_{i2}R_{i3}}{3vv_S\sin(\beta)} + \frac{\delta_{25}'}{3})2v^2s_\beta^2) + \frac{\sum_{i=1}^{3} m_i^2 R_{i3}^2}{vv_S}]R_{j3},
\end{aligned}$$

- Quartic couplings:

$$\begin{aligned}
\lambda_{h_j h_k A_S A_S} = &[\frac{\sum_{i=1}^{3} m_{h_i}^2 R_{i1}R_{i3}}{3vv_S\cos(\beta)} + \frac{4\delta_{14}'}{3}]R_{j1}R_{k1} \\
&+ [\frac{\sum_{i=1}^{3} m_{h_i}^2 R_{i2}R_{i3}}{3vv_S\sin(\beta)} + \frac{4\delta_{25}'}{3}]R_{j2}R_{k2} \\
&- [\frac{2}{v_S^2}(2m_S'^2 + m_{A_S}^2 + (\frac{\sum_{i=1}^{3} m_{h_i}^2 R_{i1}R_{i3}}{3vv_S\cos(\beta)} + \frac{\delta_{14}'}{3})2v^2c_\beta^2 \\
&+ (\frac{\sum_{i=1}^{3} m_{h_i}^2 R_{i2}R_{i3}}{3vv_S\sin(\beta)} + \frac{\delta_{25}'}{3})2v^2s_\beta^2) + \frac{\sum_{i=1}^{3} m_i^2 R_{i3}^2}{v_S^2}]R_{j3}R_{k3}.
\end{aligned}$$

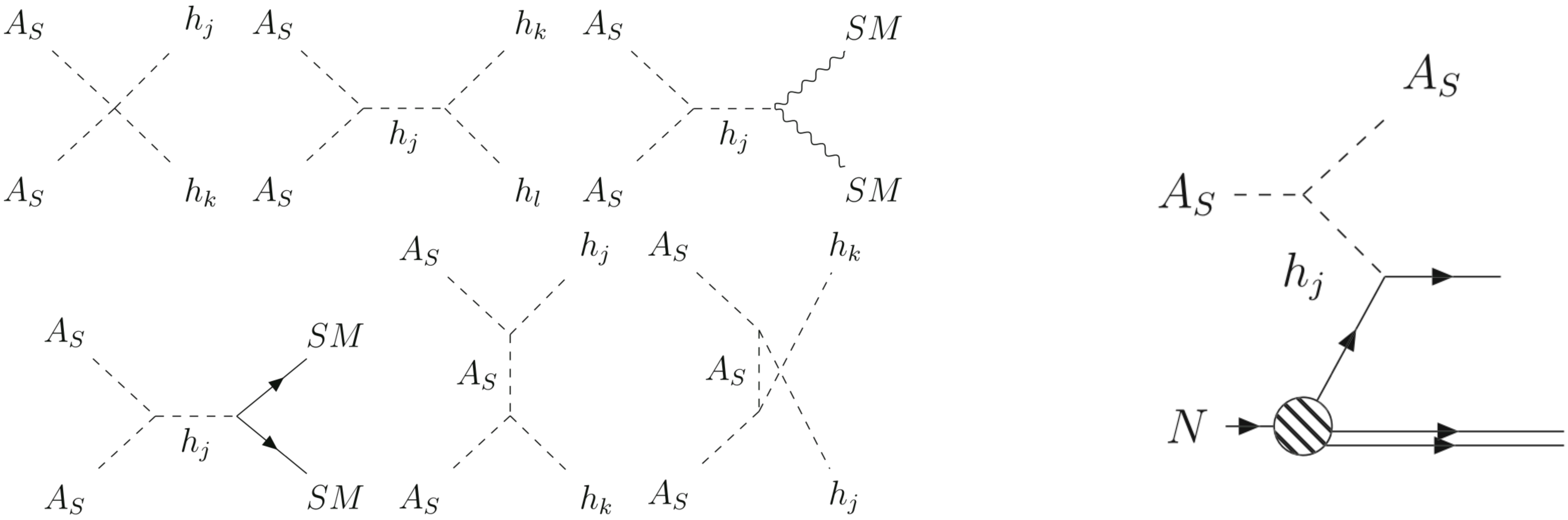

Tree level Feynman diagrams relevant for relic density and direct detection cross-section calculations

Constraints

- Model building: SARAH
- Perturbative unitarity, boundedness-from-below, vacuum stability $\Longrightarrow$ SPheno, Python, EVADE
- Relic density (mediated by quartic $A_S A_S h_i h_j$ vertices, s-channel higgses and t-channel A_S mediated contributions) upper limit from PLANCK, $\Omega h^2 = 0.1191 \pm 0.0010$, $\Longrightarrow$ micrOmegas
- Spin-independent DM-nucleon direct detection cross-section (mediated by s-channel higgses) from LUX-ZEPLIN $\Longrightarrow$ micrOmegas
- Indirect detection cross-section from DM annihilation (via higgses) from FERMI-LAT $\Longrightarrow$ micrOmegas
- Higgs mass ($\sim$125 GeV), signal strengths, and heavy Higgs search constraints $\Longrightarrow$ HiggsTools
- 95 GeV excess constraints on signal strengths from $\gamma\gamma$ (~2.9σ CMS), LEP ($b\bar{b}$, ~2.3σ LEP)

Key Features

- We consider the type II 2HDM extended with a complex singlet scalar. For the case where the real part of the complex scalar obtains a vacuum expectation value enabling a mixing between its scalar component and the 2HDM higgs sector.

- The pseudo scalar component stabilized under a Z_2' symmetry and constitutes DM candidate A_S. The higgs sector consists of $h_1, h_2, h_3, A, H^{\pm}$. The lightest Higgs set to 95 GeV while second-lightest Higgs set to 125 GeV SM-like Higgs.

- Stringent constraints on tan $\beta, \alpha_1, \alpha_2$ from constraints to fit 95 GeV in bb, $\gamma\gamma$ mode.

- Stringent constraint from boundedness-from-below, direct detection data, indirect detection data from FERMI-LAT $\Longrightarrow$ constrains the DM portal couplings parameter space while being consistent with the 95 GeV excess.

Interplay of DM and 95 GeV Higgs

m_{h_1}	m_{h_2}	m_{h_3}	m_A	m_{A_S}
95 GeV	125.09 GeV	900 GeV	900 GeV	325.86 GeV
$m_{H^\pm}$	m'^2_S	δ'_{14}	δ'_{25}	$\tan(\beta)$
900 GeV	$-4.809 \times 10^4\,\mathrm{GeV}^2$	-9.6958	0.2475	10
v_S	$c_{h_1 bb}$	$c_{h_1 tt}$	$alignm$	$\tilde{\mu}^2$
239.86 GeV	0.2096	0.4192	0.9998	$8.128 \times 10^5\,\mathrm{GeV}^2$

Benchmark point **BP1**

Parameters	Range
$c_{h_1 bb}$	$[0.0996, 0.320]$
$c_{h_1 tt}$	$[0.309, 0.529]$

Parameter ranges for the couplings to fit the 95 GeV excess.

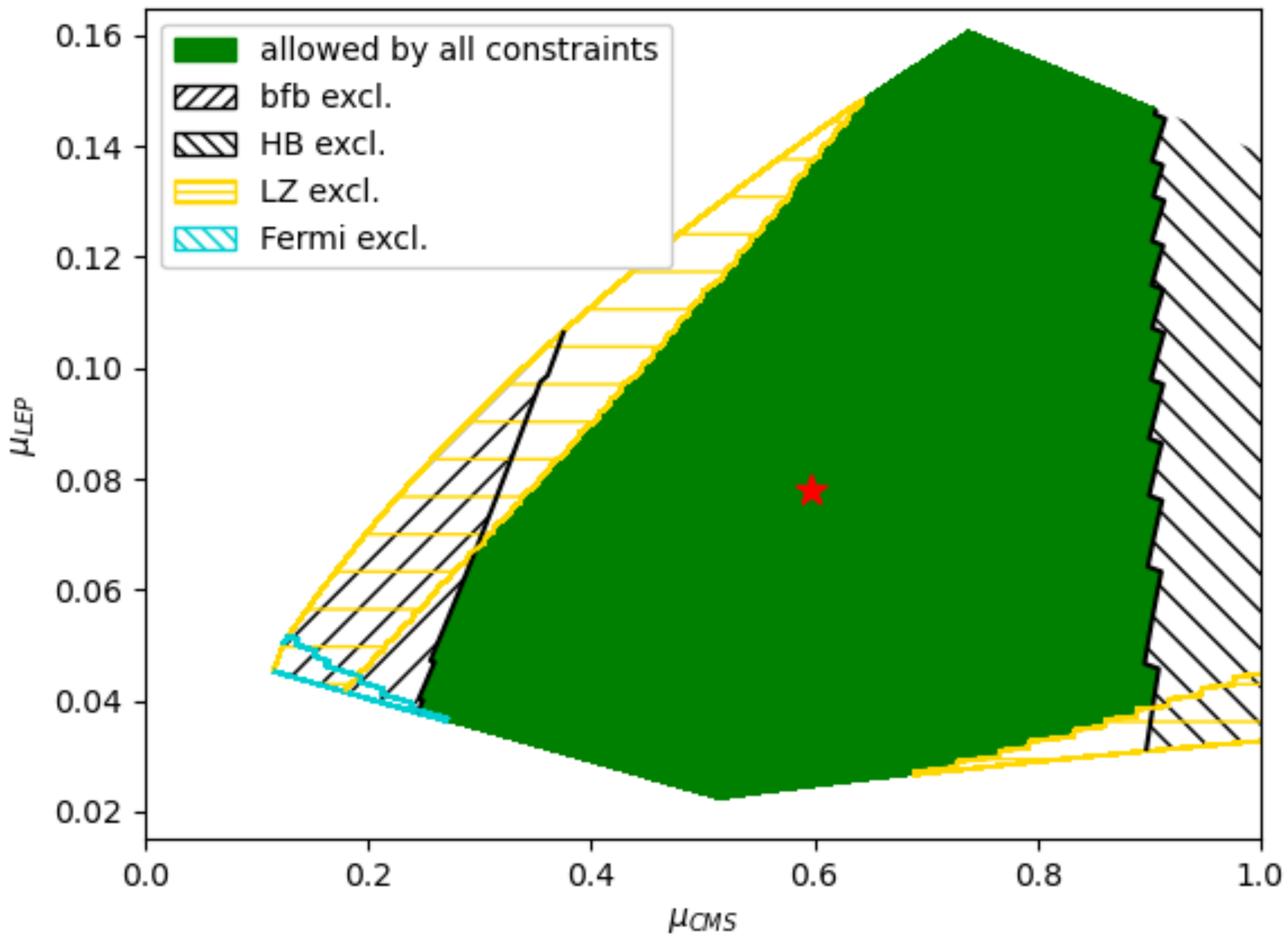

Allowed region consistent with 95 GeV excess, theoretical and experimental constraints from Higgs and dark matter searches.

S.Heinemeyer et.al,
Phys. Rev. D 106 (2022), no. 7 075003

Salient Features from DM observables

- Cancellations between contributions from $h_1$and h_2 (blue line).
- Dominant DM annihilation from Di-higgs,WW and bb channels.
- DM relic density mostly under abundant over the scanned parameter space.

Conservative limits placed from LZ and FERMI-LAT.

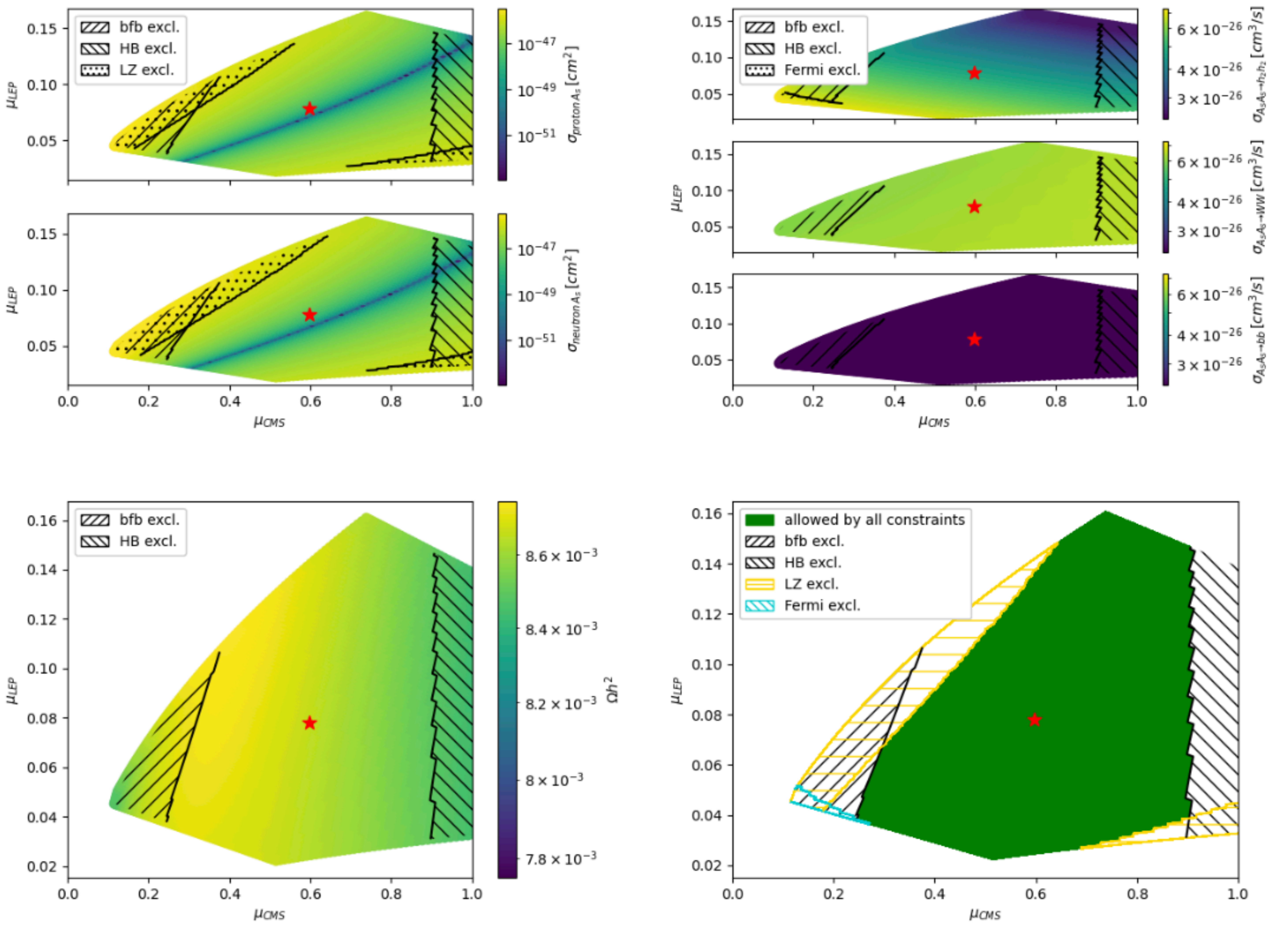

Constraints on $\delta'_{14} - \delta'_{25}$

$$\delta'_{14} = \lambda'_4 - \lambda'_1,$$
$$\delta'_{25} = \lambda'_5 - \lambda'_2.$$

- Stringent constraints from LZ and Fermi-LAT data as well from boundedness-from-below constraints.

$$\frac{\lambda_{h_j A_S A_S}}{v} = [\frac{\sum_{i=1}^{3} m_{h_i}^2 R_{i1} R_{i3}}{3 v v_S \cos(\beta)} + \frac{4\delta'_{14}}{3}] c_\beta R_{j1}$$
$$+ [\frac{\sum_{i=1}^{3} m_{h_i}^2 R_{i2} R_{i3}}{3 v v_S \sin(\beta)} + \frac{4\delta'_{25}}{3}] s_\beta R_{j2}$$
$$- [\frac{2}{v v_S}(2 m'^2_S + m^2_{A_S} + (\frac{\sum_{i=1}^{3} m_{h_i}^2 R_{i1} R_{i3}}{3 v v_S \cos(\beta)} + \frac{\delta'_{14}}{3}) 2 v^2 c_\beta^2$$
$$+ (\frac{\sum_{i=1}^{3} m_{h_i}^2 R_{i2} R_{i3}}{3 v v_S \sin(\beta)} + \frac{\delta'_{25}}{3}) 2 v^2 s_\beta^2) + \frac{\sum_{i=1}^{3} m_i^2 R_{i3}^2}{v v_S}] R_{j3},$$

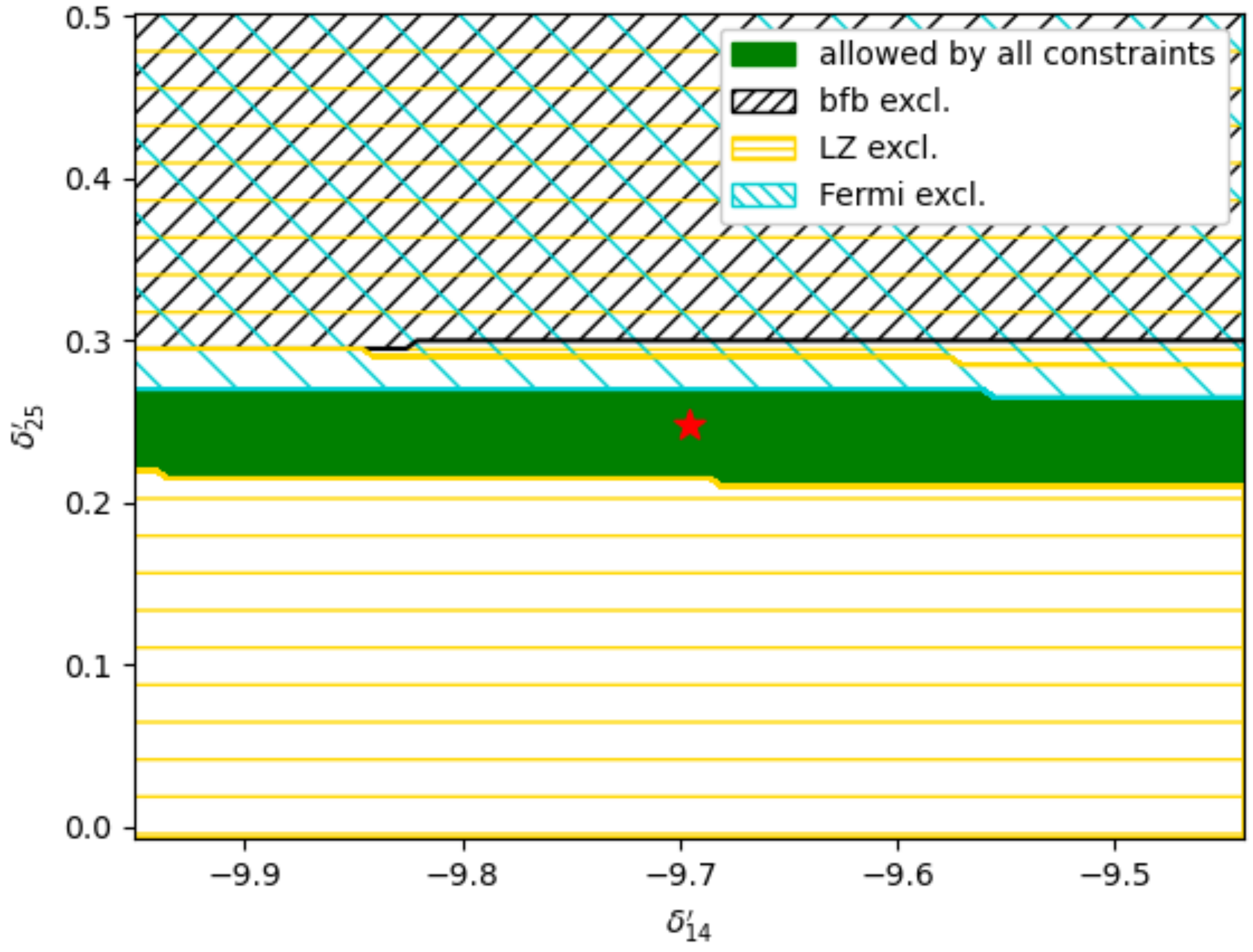

Allowed by all constraints.

Effect of δ'_{25} dominant δ'_{14}over due to multiplicative factor of $\sin\beta$.

Salient Features: $m_S^{2'} - m_{A_S}$ variation

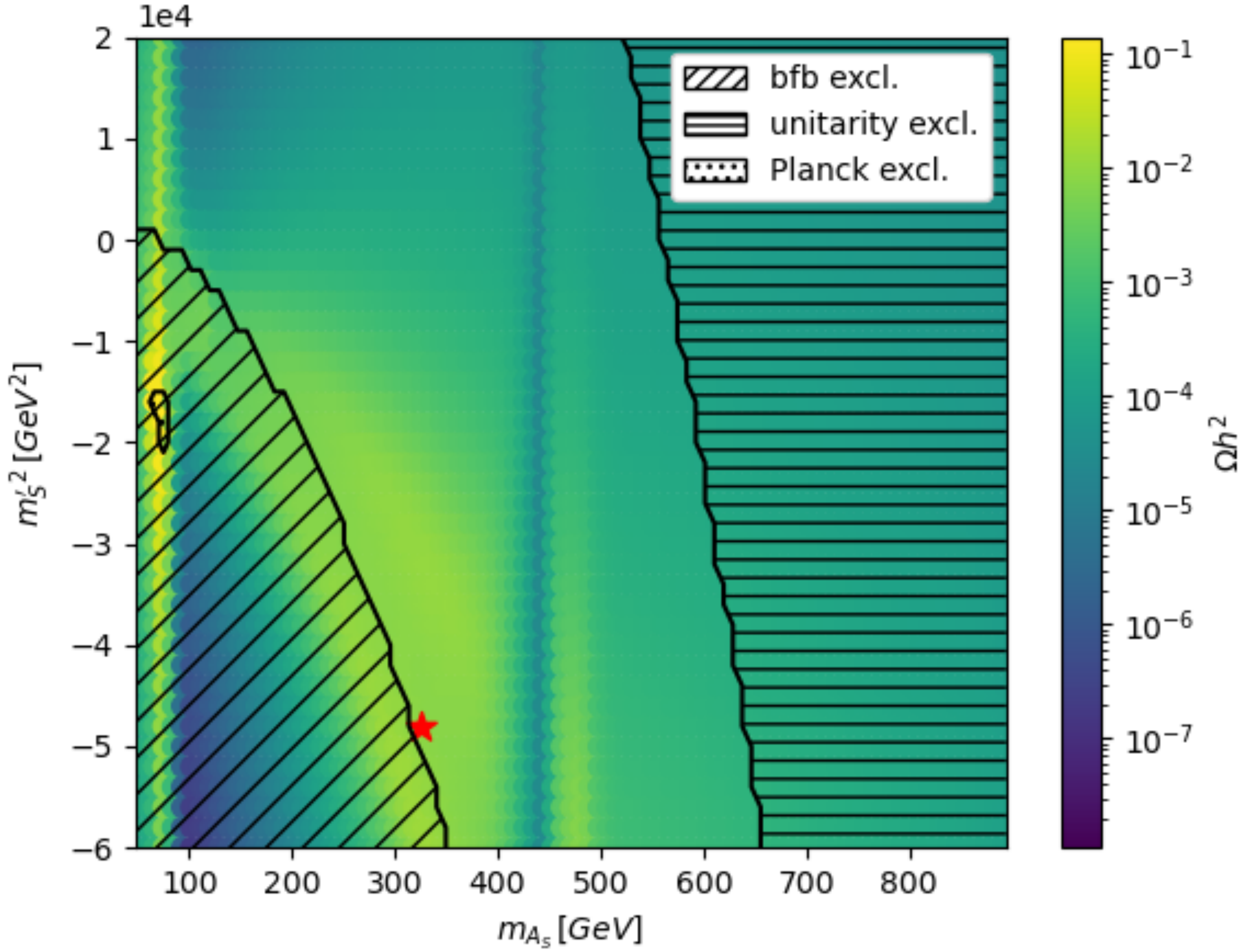

Effect of Relic density constraints.

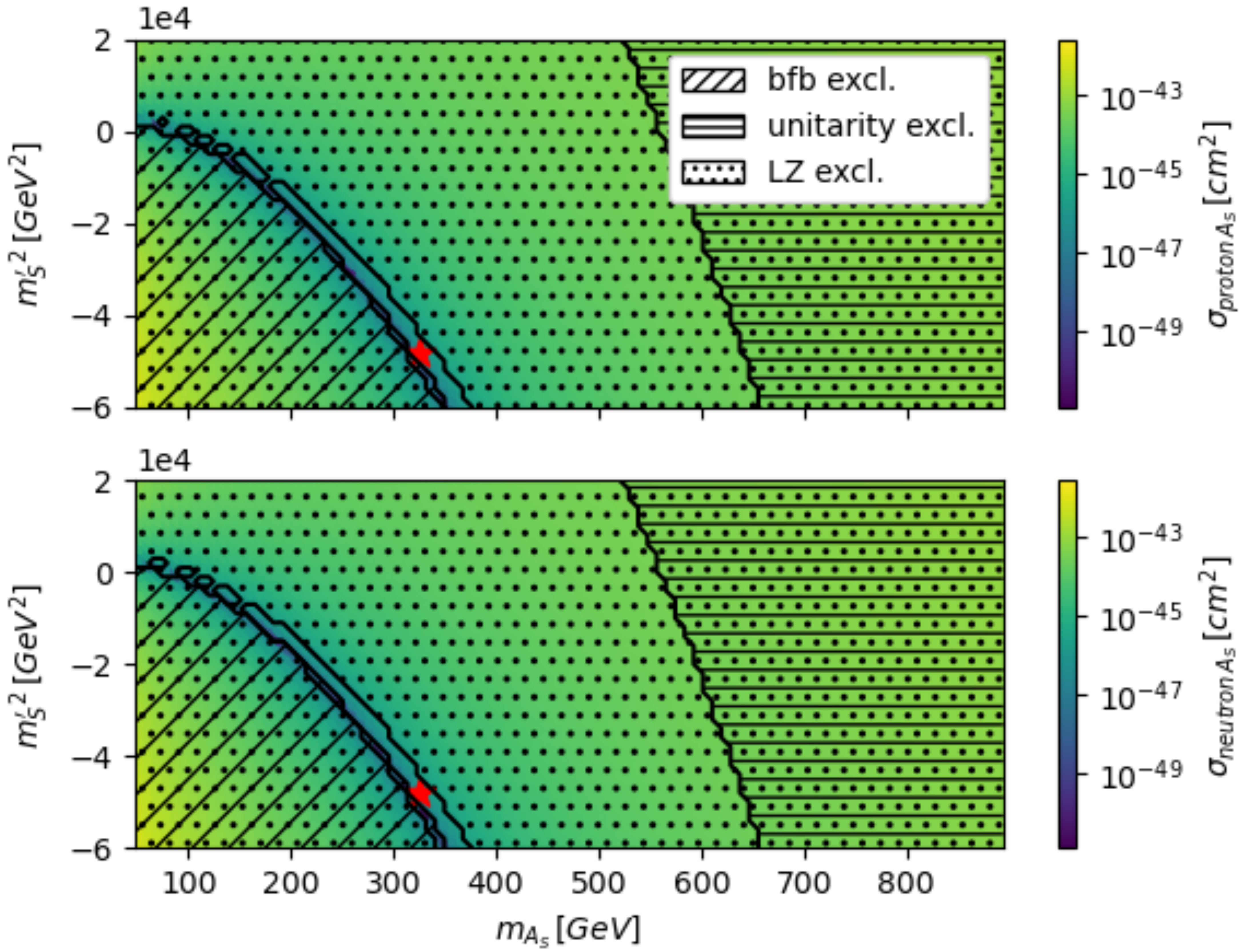

Effect of LZ constraints.

- Dips observed at $m_{A_S} \sim 62{,}450 GeV$ corresponding to SM Higgs and heavy Higgs resonant regions.
- LZ stringently rules out much of the parameter space for $m_S^{2'} - m_{A_S}$ plane.

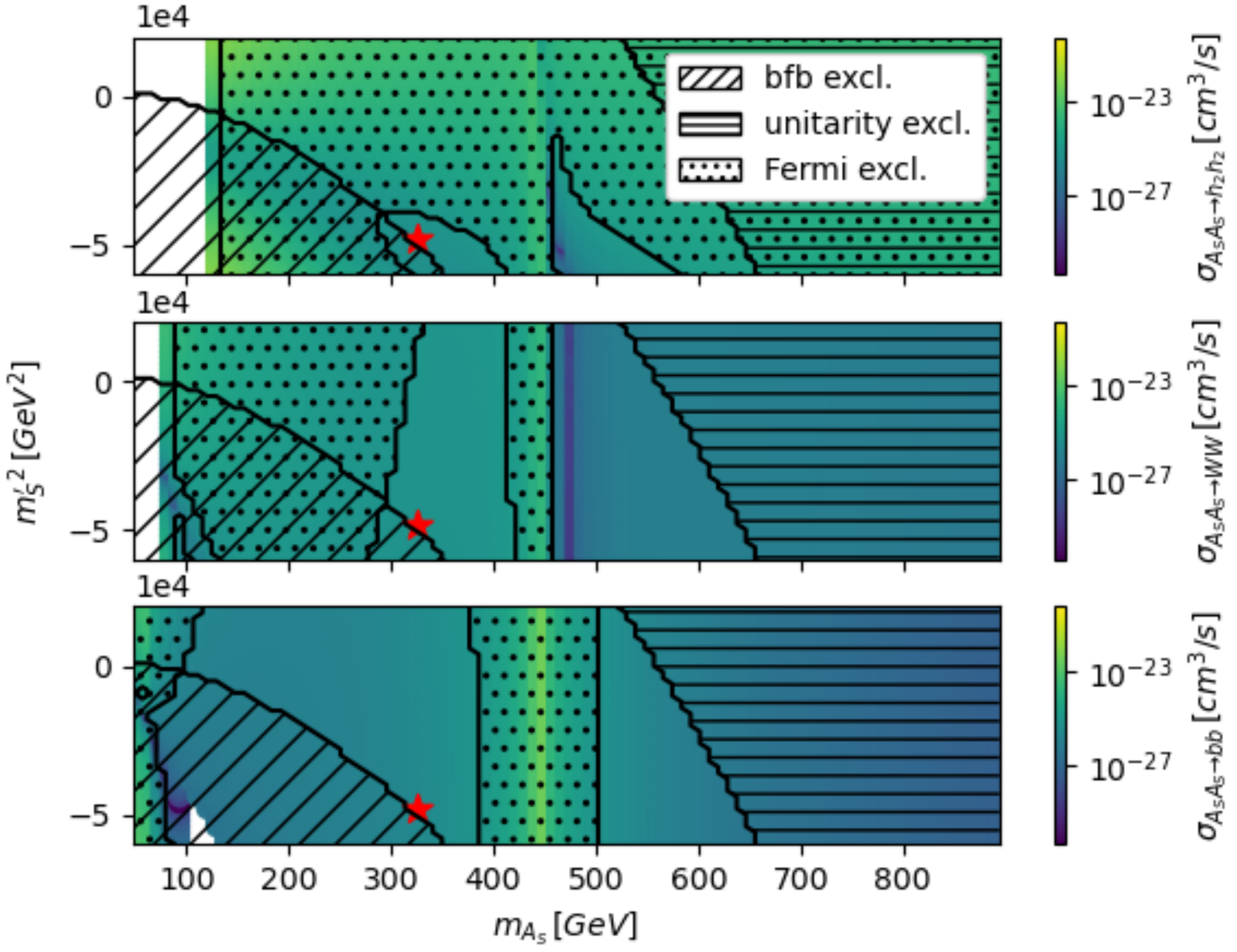

Effect of FERMI-LAT constraints.

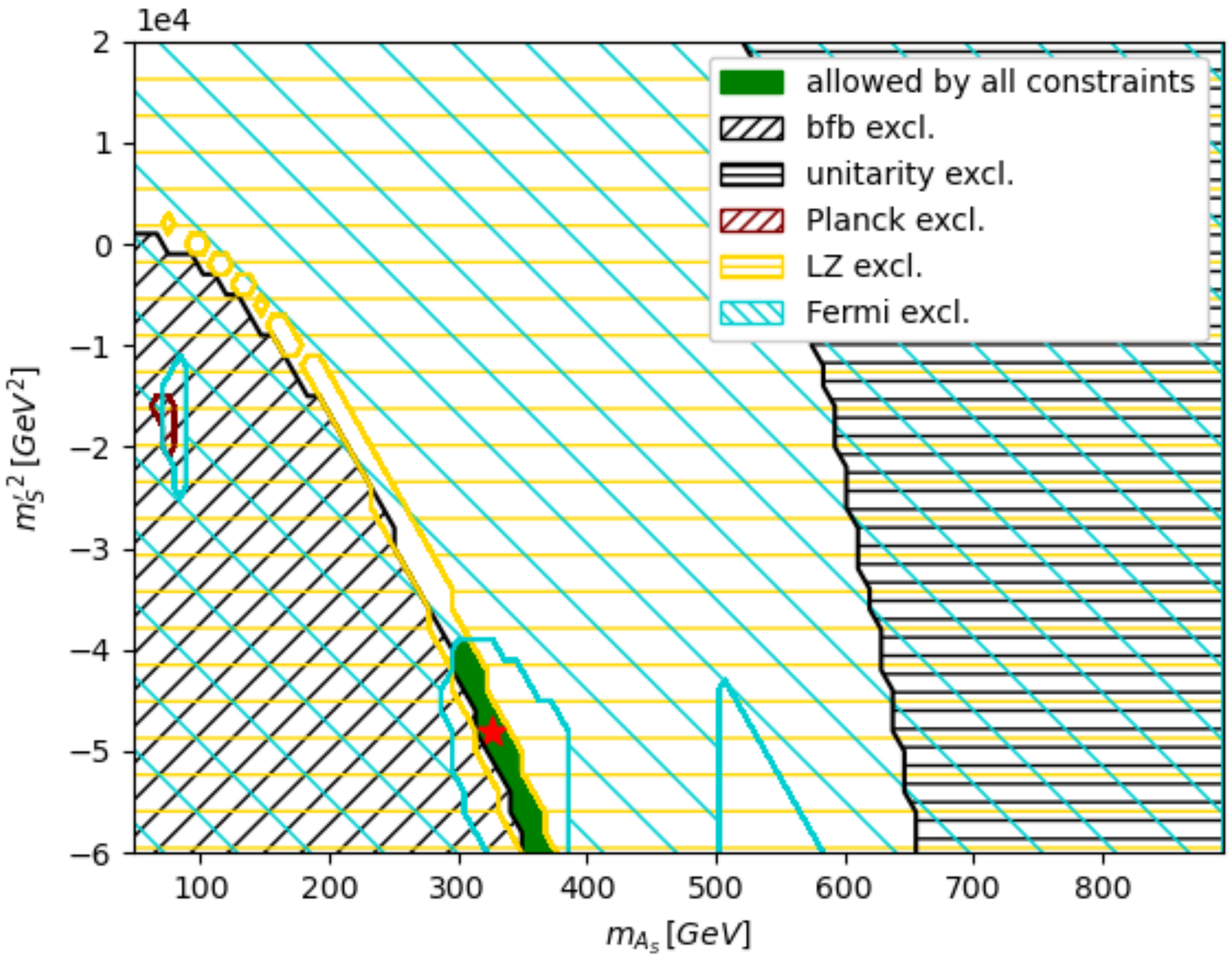

Allowed parameter space.

- Dominant annihilation channel via $h_2 h_2$ followed by WW and $b\bar{b}$.
- Strong dip in DM DM -> W W channel at ~475 GeV due to proliferation of $b\bar{b}$, $h_1 h_1$, $h_1 h_2$, $t\bar{t}$ channels.
- Constraints arise on other parameter variations, particularly from varying $\delta'_{14} - \delta'_{25}$, $\delta'_{25} \simeq 0.25$ to satisfy constraints from LZ => allowed region from cancellations between $h_1$and h_2.

Preliminary results.

m_{h_1}	m_{h_2}	m_{h_3}	m_A	$m_{H^\pm}$
95.4 GeV	125.09 GeV	700 GeV	700 GeV	700 GeV
m_{A_S}	$m_S'^2$	δ'_{14}	δ'_{25}	$\tan(\beta)$
325.86 GeV	-4.809×10^4 GeV^2	-9.6958	0.2475	6.6
v_S	c_{h_1bb}	c_{h_1tt}	$alignm$	$\tilde{\mu}$
239.86 GeV	0.258	0.372	0.9998	700 GeV

Table 3. The benchmark point **BP2** in the mass basis

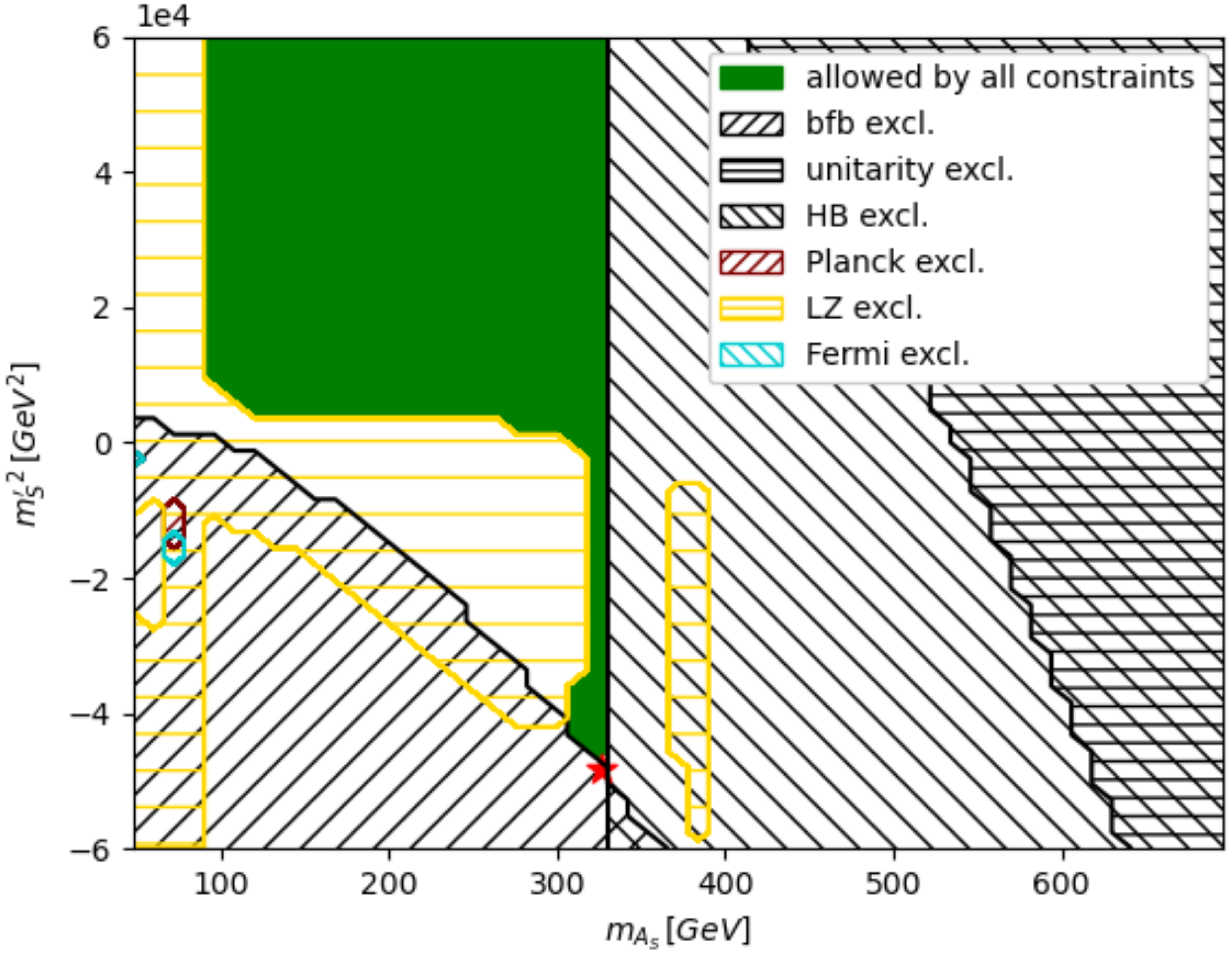

Allowing for rescaling with the PLANCK measured relic density opens up the parameter space considerably. (Red Star: BP2).

Collider Phenomenology

- The presence of a dark matter candidate allows new decay modes for the heavy Higgs h_3 to open up $\Longrightarrow$ Missing energy signals at colliders!

Decay Modes	Branching Ratio (BR)
$h_3 \to b\bar{b}$	0.412
$h_3 \to A_S A_S$	0.247
$h_3 \to t\bar{t}$	0.106
$h_3 \to \tau\tau$	0.064
$h_3 \to h_2 h_2$	0.061
$h_3 \to h_1 h_2$	0.035
$h_3 \to h_1 h_1$	0.022

Decay modes for h_3 in BP1.

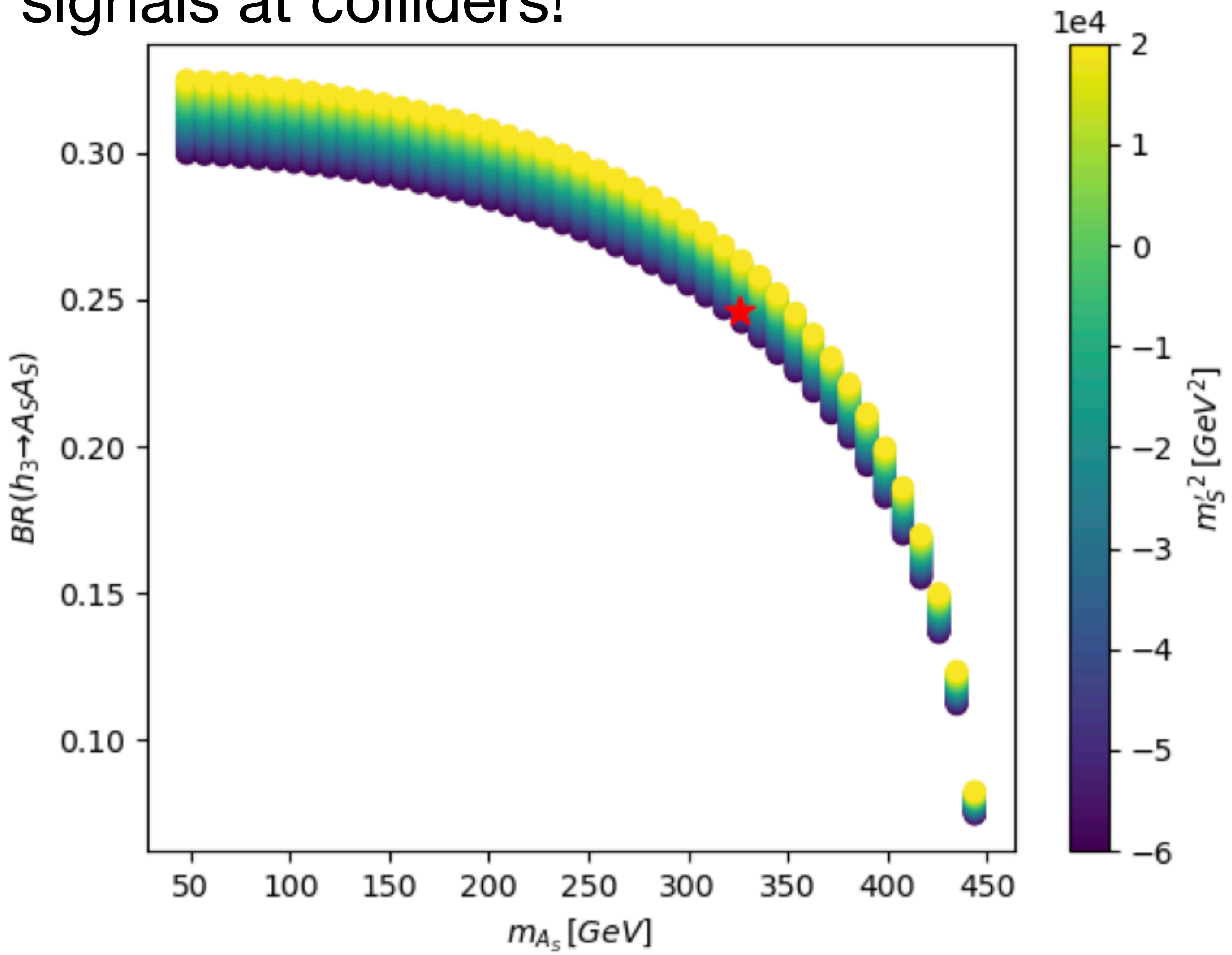

Variation of BR($h_3 \to A_S A_S$) vs. DM mass for BP1 and Higgs constraints

Signals at HL-LHC

- Signal: Mono-jet + MET $\sigma_{GGF} \times BR(h_3 \times A_S A_S) = 0.232\ \text{fb}$ for m_{h_3}=900 GeV.

Using cuts:

C1 : $N_j <= 4, p_T(j) > 30$ GeV, $\eta < 2.8$, C2 : $\not{E}_T > 250$ GeV,
C3 : $p_T(j_1) > 250$ GeV C4:$\Delta\Phi(j, \not{E}_T) > 0.4$,$\Delta\Phi(j_1, \not{E}_T) > 0.6$, C5 : $N_\ell = 0$,

signal significance = 1.36(LO) and 2.6σ (NNLO+NNLL).

Process	C1	C2	C3	C4	C5
GGF	696	137	114	114	114
$\mathcal{S}$			$1.356\,\sigma$		

The cut flow table for BP1 for signal events at HL-LHC ($\sqrt{s} = 14$ TeV and 3000fb^{-1})

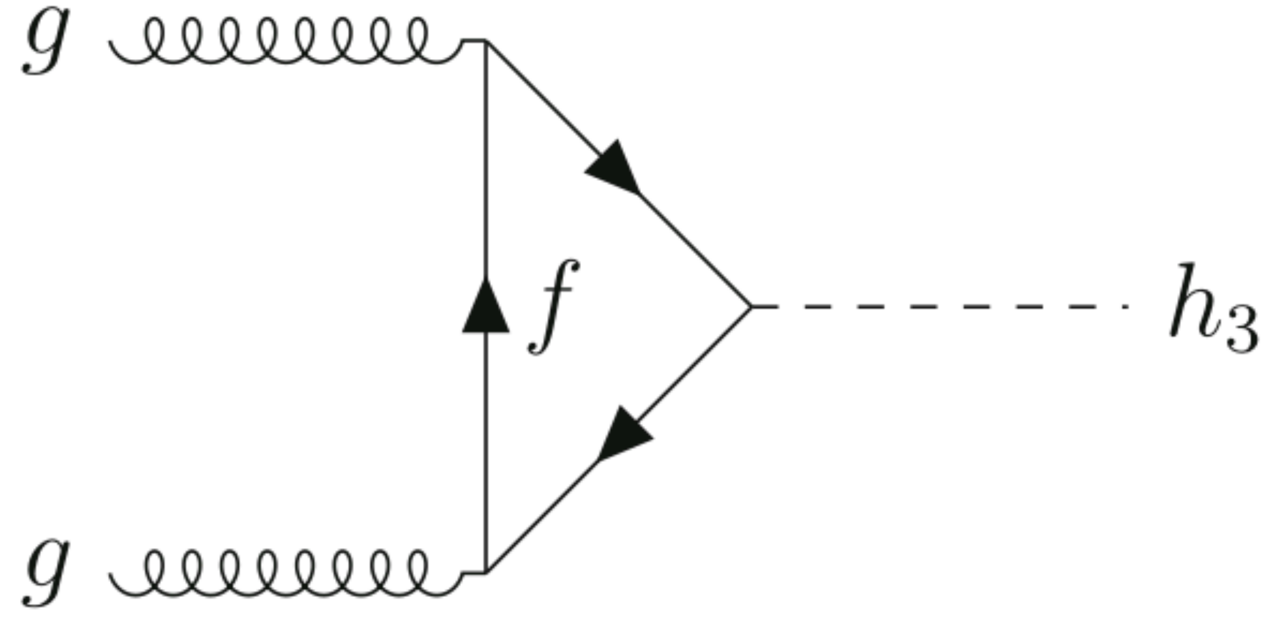

Gluon Fusion (GGF)

Cuts from JHEP 01 (2018) 126

- Signal: 2 forward jets + $\not{E}_T$
  $\sigma_{VBF} \times BR(h_3 \to A_S A_S)= 0.011$ fb.

- Using cuts:

D1: $p_T(j_1) > 80$ GeV, $p_T(j_2) > 40$ GeV, $\Delta\Phi(j, \not{E}_T > 0.5,$

D2: $\eta_{j_1 j_2} < 0, \Delta\Phi_{j_1 j_2} < 1.5,$ D3: $\Delta\eta_{j_1, j_2} > 3.0,$ D4: $M_{j_1 j_2} > 600$ GeV, D5: $\not{E}_T > 200$ GeV, D6: $N_\ell = 0,$

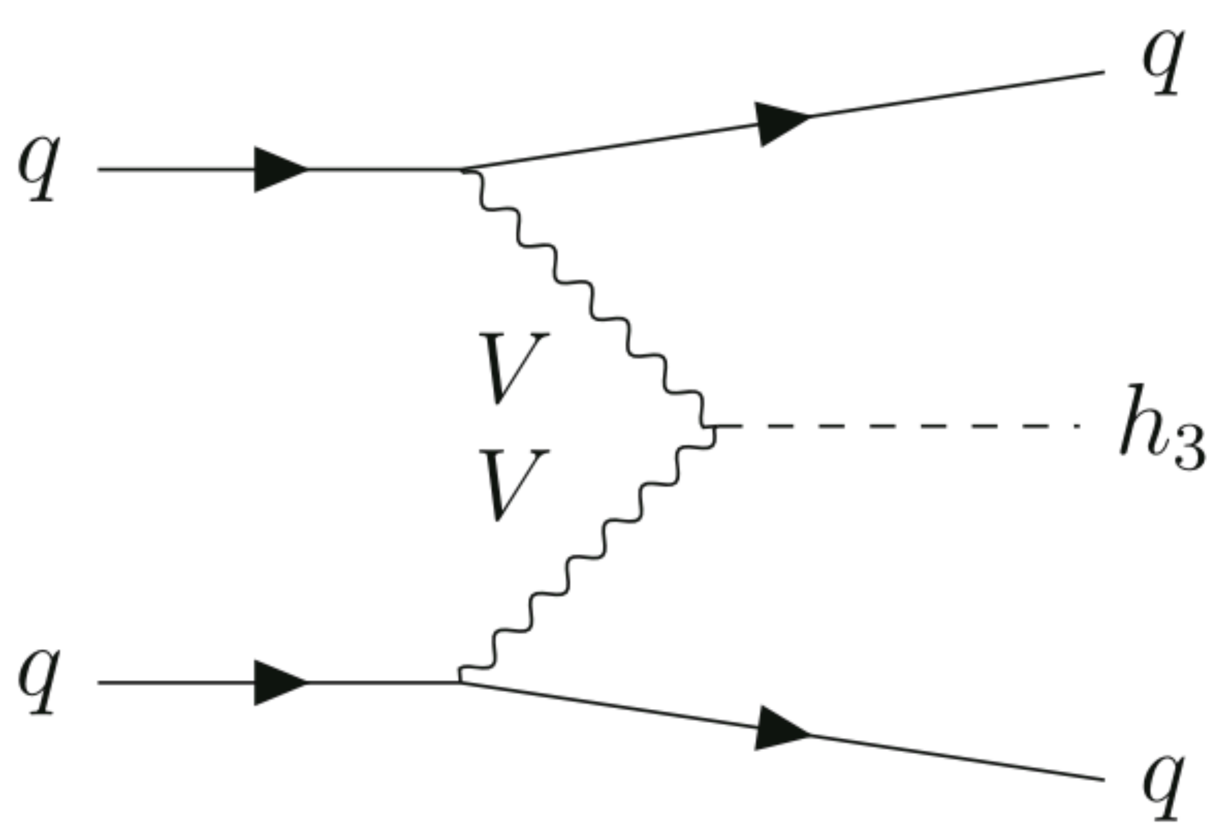

Vector Boson Fusion (VBF)

signal significance = 0.0032σ (LO) and $0.0055\ \sigma$ (NNLO).

Process	D1	D2	D3	D4	D5	D6
VBF	1.25	0.27	0.11	0.11	0.11	0.11
$\mathcal{S}$			$0.0032\ \sigma$			

The cut flow table for BP1 for signal events at HL-LHC ($\sqrt{s} = 14$ TeV and 3000fb^{-1}.)

Signals at lepton colliders

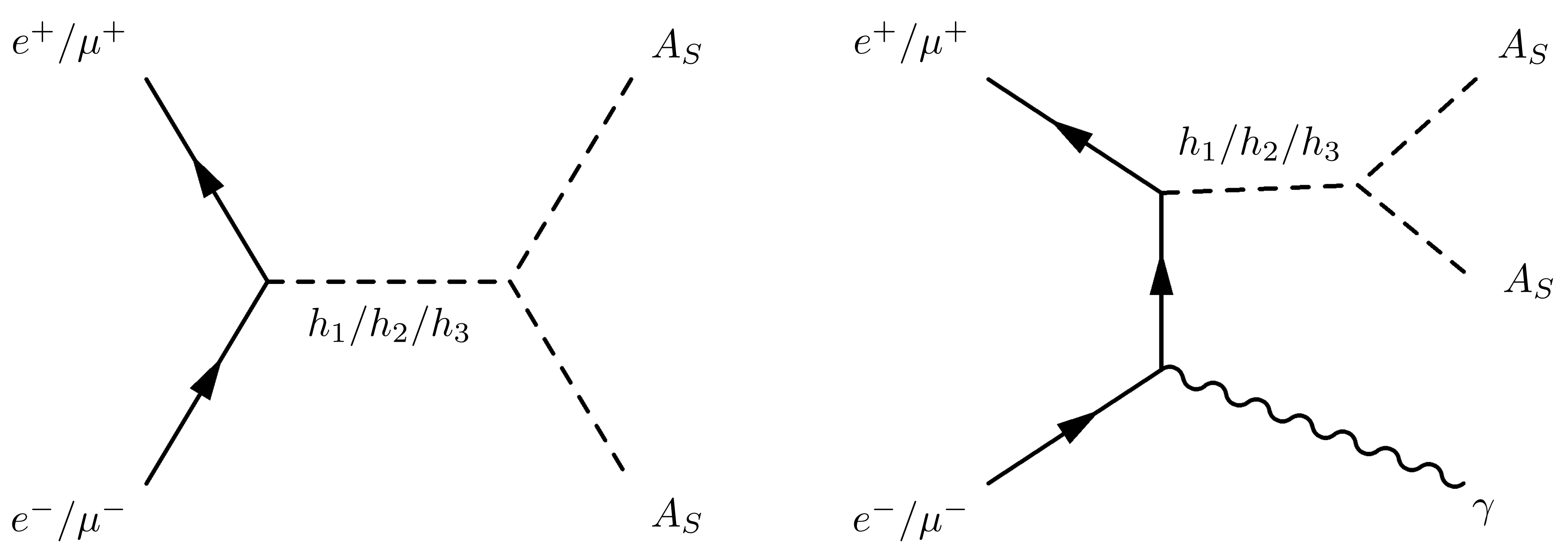

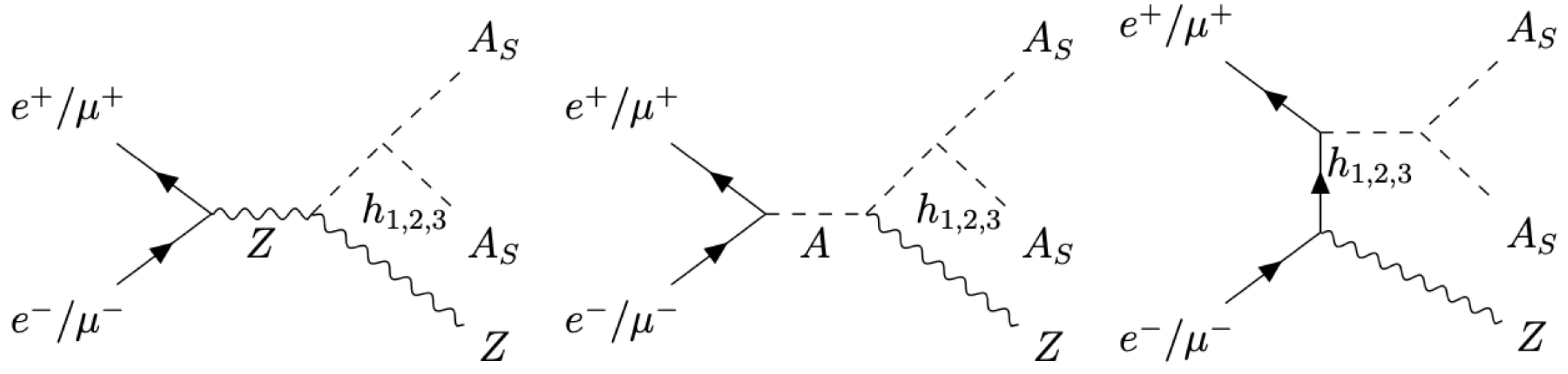

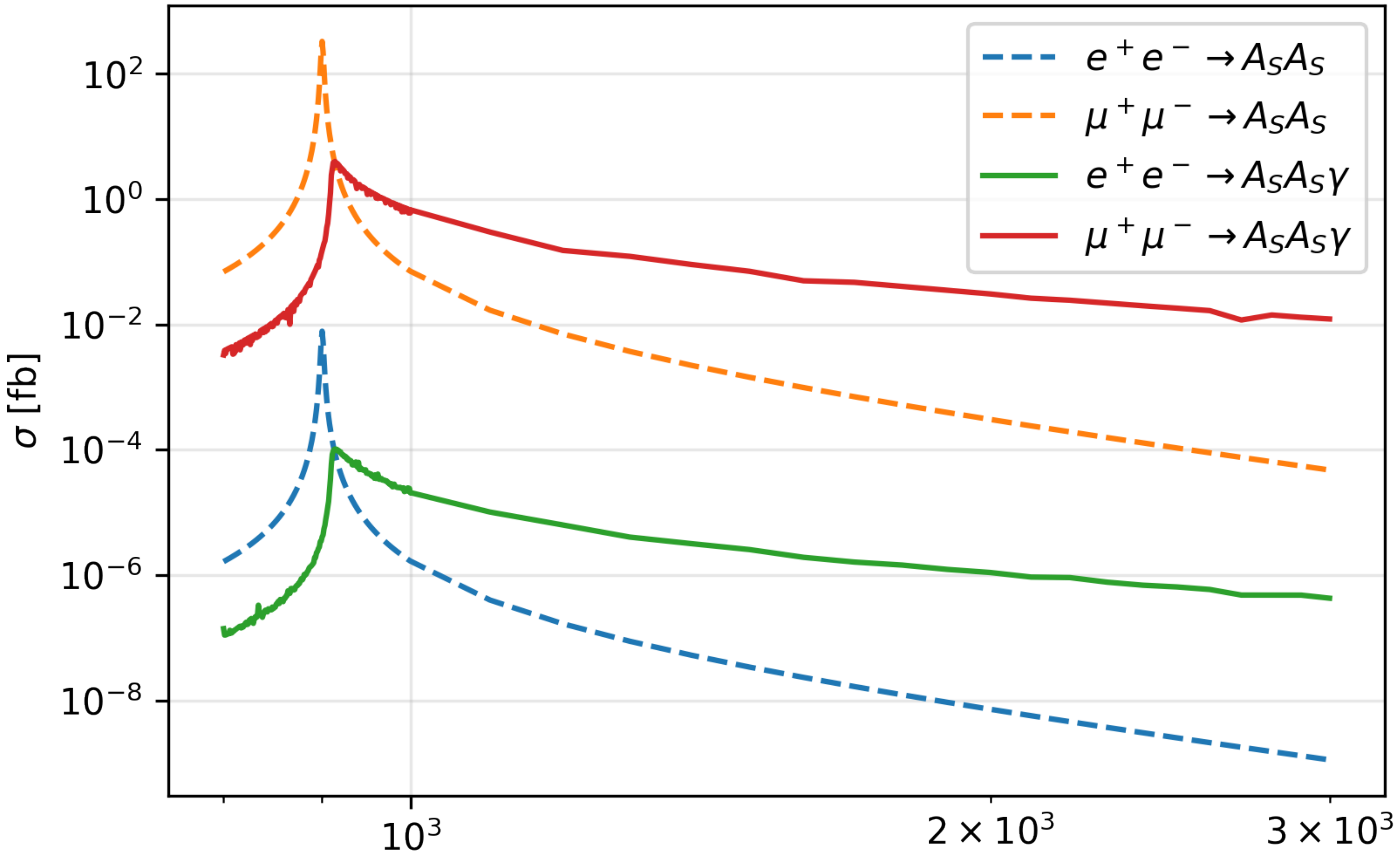

Mono-photon + Missing Energy

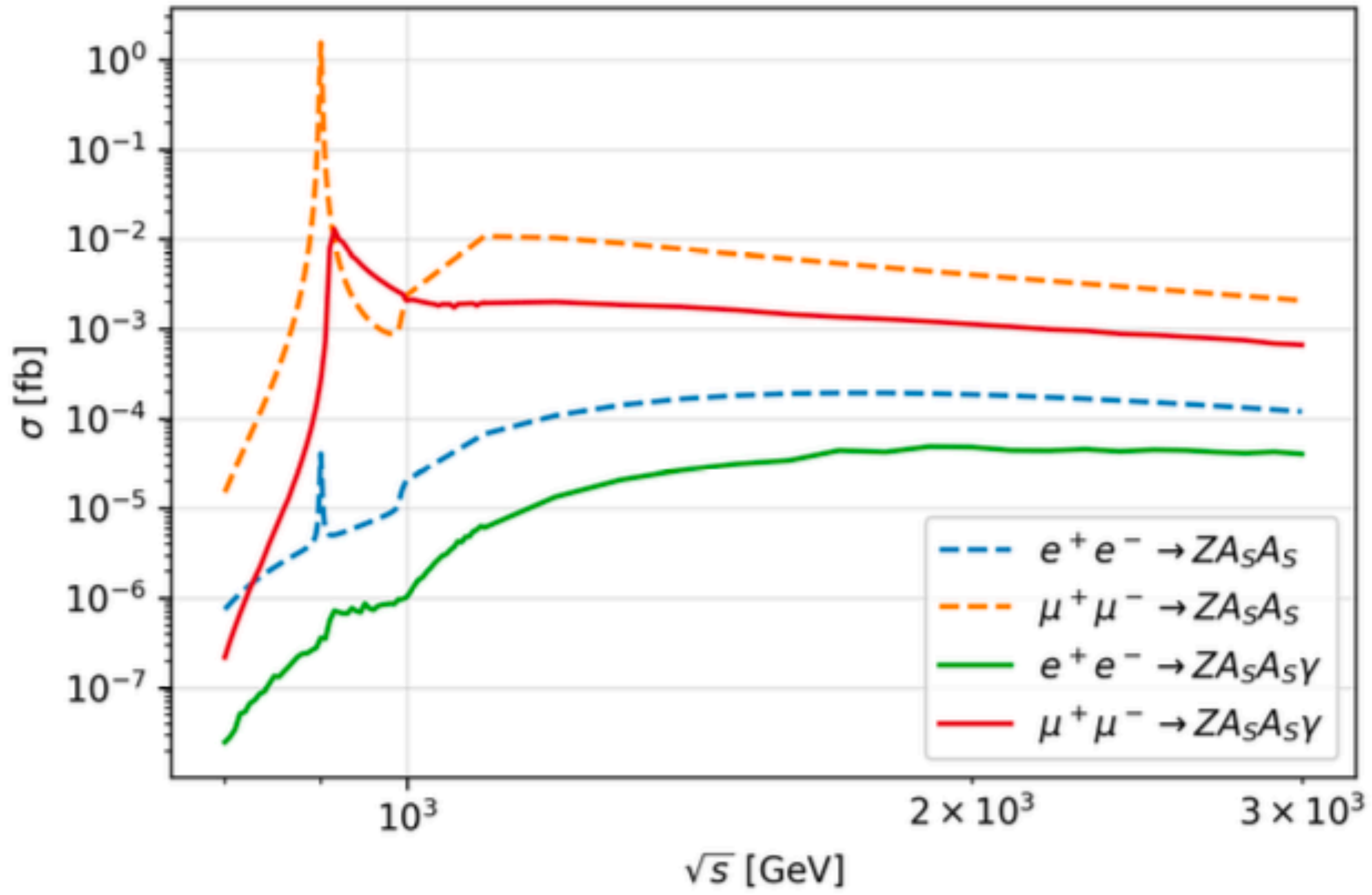

Mono-Z + Missing Energy

Significant enhancements near the higgs resonance region observed in muon colliders due to the muon Yukawa coupling $\Longrightarrow$ complementary searches to LHC.

Preliminary results.

Benchmarks

	m_{h_3} (GeV)	m_χ (GeV)	Ωh^2	σ_{pA_S}/pb	$\sigma_{A_S A_S \to XX}/\frac{\mathrm{cm}^3}{\mathrm{s}}$	$BR(h_3 \to \chi\chi)$	$BR(h_2 \to \chi\chi)$
BP1	900	325.86	8.71×10^{-3}	4.402×10^{-12}	1.696×10^{-27}	0.25	-
BP2	700	325.86	3.16×10^{-4}	6.033×10^{-12}	1.458×10^{-29}	0.48	-
BP3	700	156.0	1.61×10^{-4}	3.903×10^{-11}	3.875×10^{-29}	0.69	-
BP55	650	55.6	0.11	4.21×10^{-12}	1.98×10^{-28}	3.81×10^{-9}	0.0199
BP2900	2900	1000	0.111	3.323×10^{-11}	2.045×10^{-26}	0.0359	-

- Benchmarks chosen with thermal relic and underabundant cases satisfying all theoretical and experimental constraints.

- Possible signals at e+e- colliders as well as muon colliders.

- Signals: Mono-γ+ missing energy, Mono-Z + missing energy

- Dominant SM background: $\nu\nu\gamma, \nu\nu Z$ respectively.

Mono-γ+ missing energy:

- For BP1, with $m_{h_3} = 900$ GeV, significance ~ 2.4 σ at 10 ab^{-1}at 1 TeV muon collider.
- For BP3 with a lighter Higgs, $m_{h_3} = 700$ GeV, and higher invisible branching to DM ~ 69%, significance ~ 5.3 σat 10 ab^{-1} for a 1 TeV muon collider.

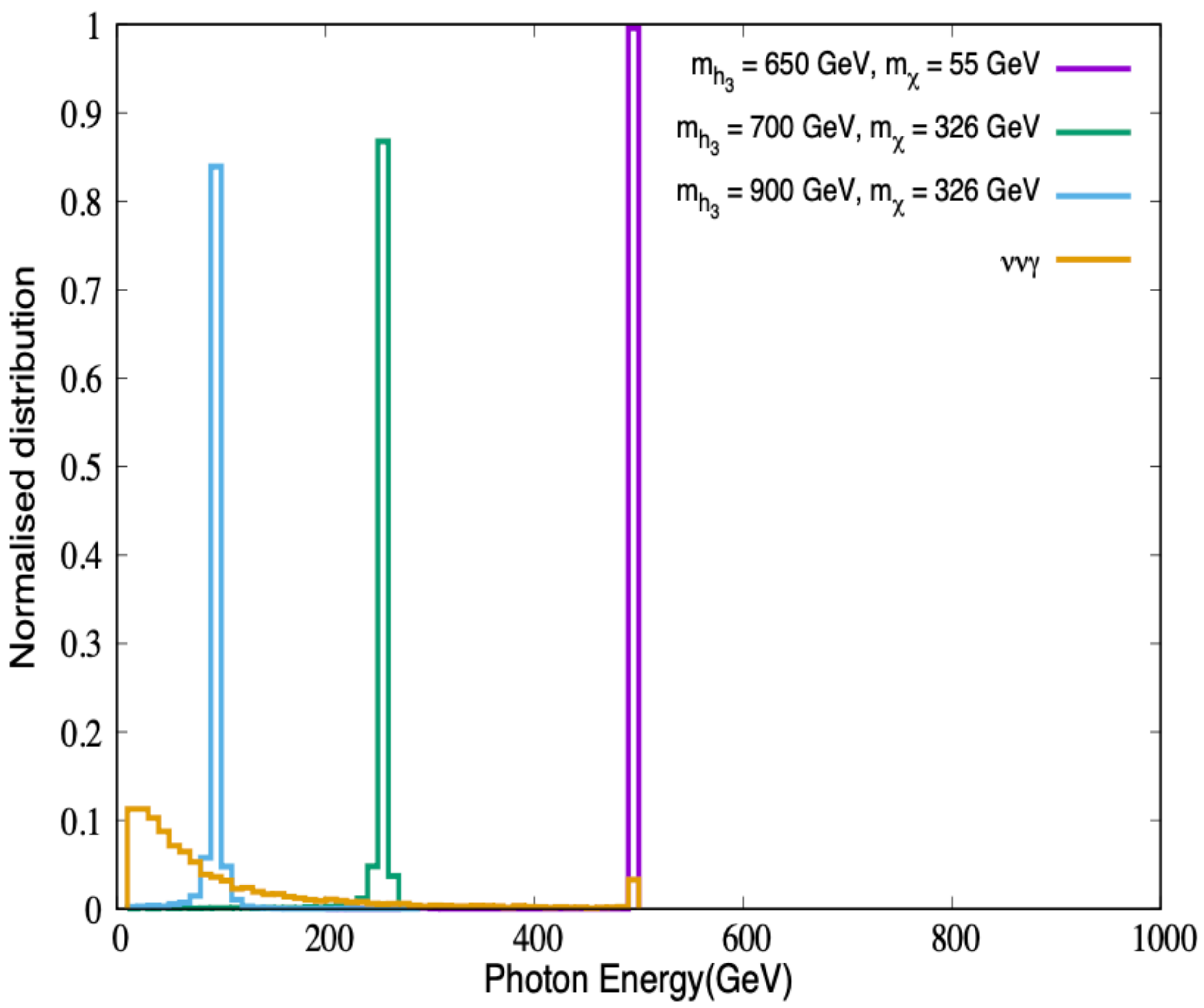

Variation of photon energy for 1 TeV muon collider.

Mono-Z + missing energy:

Preliminary results.

Benchmark	$\mathcal{S}(\sqrt{s}$=250 GeV)	$\mathcal{S}(\sqrt{s}$=500 GeV)	$\mathcal{S}(\sqrt{s}$=1 TeV)	$\mathcal{S}(\sqrt{s}$=3 TeV)
BP2900			–	0.14 (10 ab^{-1})
BP55	4.3 (1 ab^{-1}), 7.4 (3 ab^{-1})	1.2 (1 ab^{-1}), 2.0 (3 ab^{-1})	5.4 (10 ab^{-1}),	0.38 (10ab $^{-1}$)

Table 2: The signal significance of BP2900 mono-photon process at 3 TeV muon collider, and the Signal significance of BP55 at 250 GeV (ILC), 500 GeV (ILC) and 1 TeV (muon collider), 3 TeV (muon collider) in the mono-Z(leptonic) final state.

C.Li, et.al, PoS(ICHEP2024)772

BP55 with $m_{h_3} = 650$ GeV, and light DM~55 GeV and thermal relic has best significance at ILC ($\sqrt{s} = 250$ GeV) and for 1 TeV muon collider.

Benchmarks with heavier Higgs and DM masses and sensitive to higher $\sqrt{s}$ along with potential for other possible signal modes underway!

Preliminary results.

Mono-Z + missing energy:

- For BP55, significance ~ 5.3 σ at 10 ab^{-1} for 1 TeV muon collider for leptonic final state.

Useful kinematic variable: missing mass

$$\begin{aligned} \not{M} &= E_{inv}^2 - |\vec{p_{inv}}|^2 \\ &= (\sqrt{s} - E_Z)^2 - |\vec{p_Z}|^2 \\ &= (\sqrt{s} - E_Z)^2 - (E_Z^2 - m_Z^2) \\ &= s - 2\sqrt{s}E_Z + m_Z^2 \end{aligned}$$

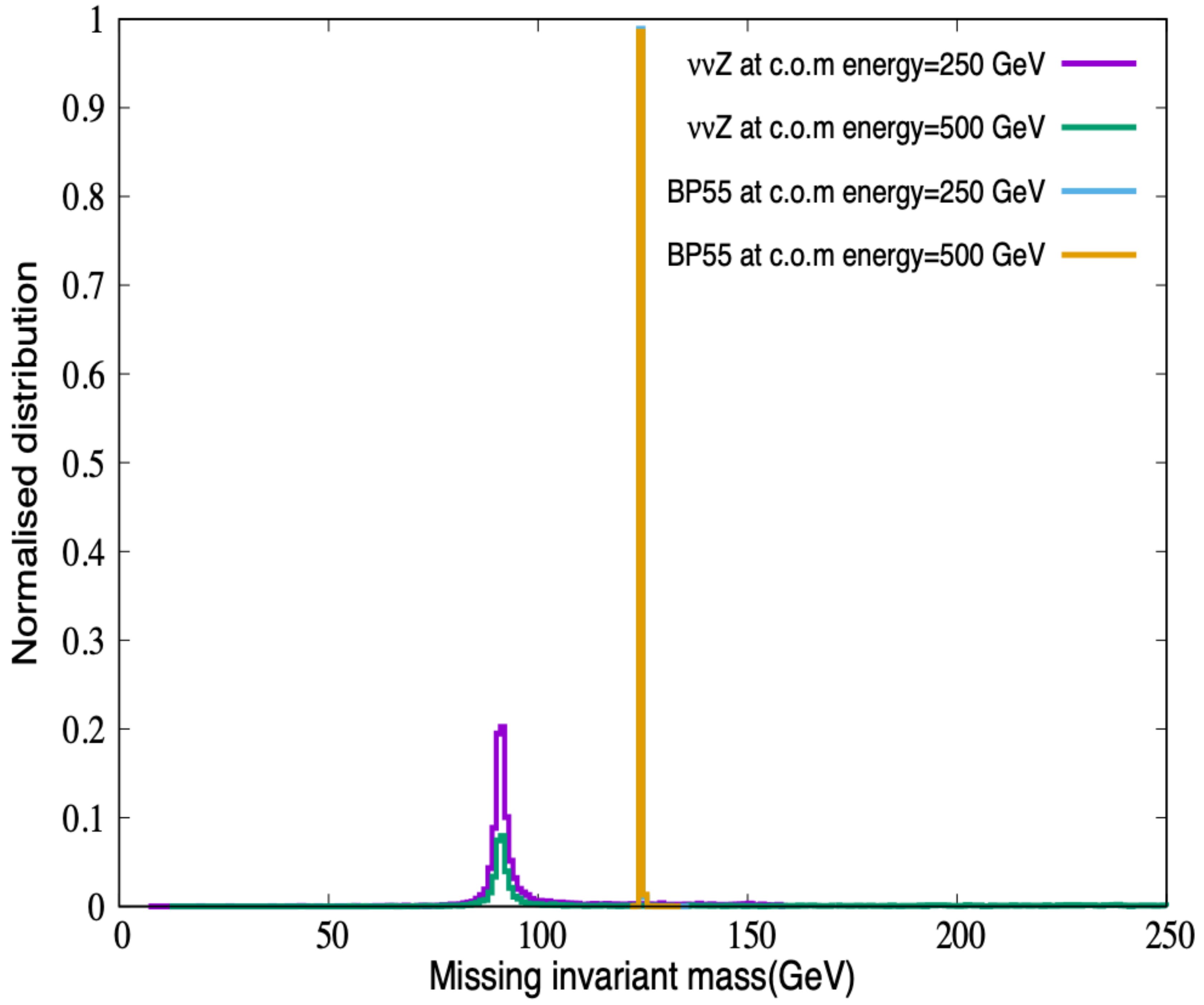

Variation of missing mass

Summary and Outlook

- We consider the type II 2HDM extended with a complex singlet scalar. For the case where the real part of the complex scalar obtains a vacuum expectation value enabling a mixing between its scalar component and the 2HDM higgs sector. The pseudo scalar component stabilized under a Z_2' symmetry and constitutes DM candidate A_S. The higgs sector consists of $h_1, h_2, h_3, A, H^{\pm}$. The lightest Higgs set to 95 GeV while second-lightest Higgs set to 125 GeV SM-like Higgs.

- Stringent constraints on $\tan\beta, \alpha_1, \alpha_2$ from constraints to fit 95 GeV in bb, $\gamma\gamma$ mode.

- Stringent constraint from boundedness-from-below, direct detection data, indirect detection data from FERMI-LAT $\Longrightarrow$ constrains the DM portal couplings parameter space while being consistent with the 95 GeV excess.

- Potential signals at LHC: Mono-jet + $\not{E}_T$ upto 2.6 σ (NNLO+NNLL) for $m_{h_3} = 900 GeV$ and BR($h_3 \to A_S A_S$) ~ 0.25. Conservative limits placed on m_{h_3}, further improvements for Di-jet + $\not{E}_T$ signals expected for lower m_{h_3}.

- Potentially exciting signals at lepton colliders: e^+e^- and $\mu^+\mu^-$ with enhancements for mono-γ and mono-Z + missing energy signals for the latter. A full collider simulation is underway to span interesting regions of the parameter space - Stay tuned!

Thank You!

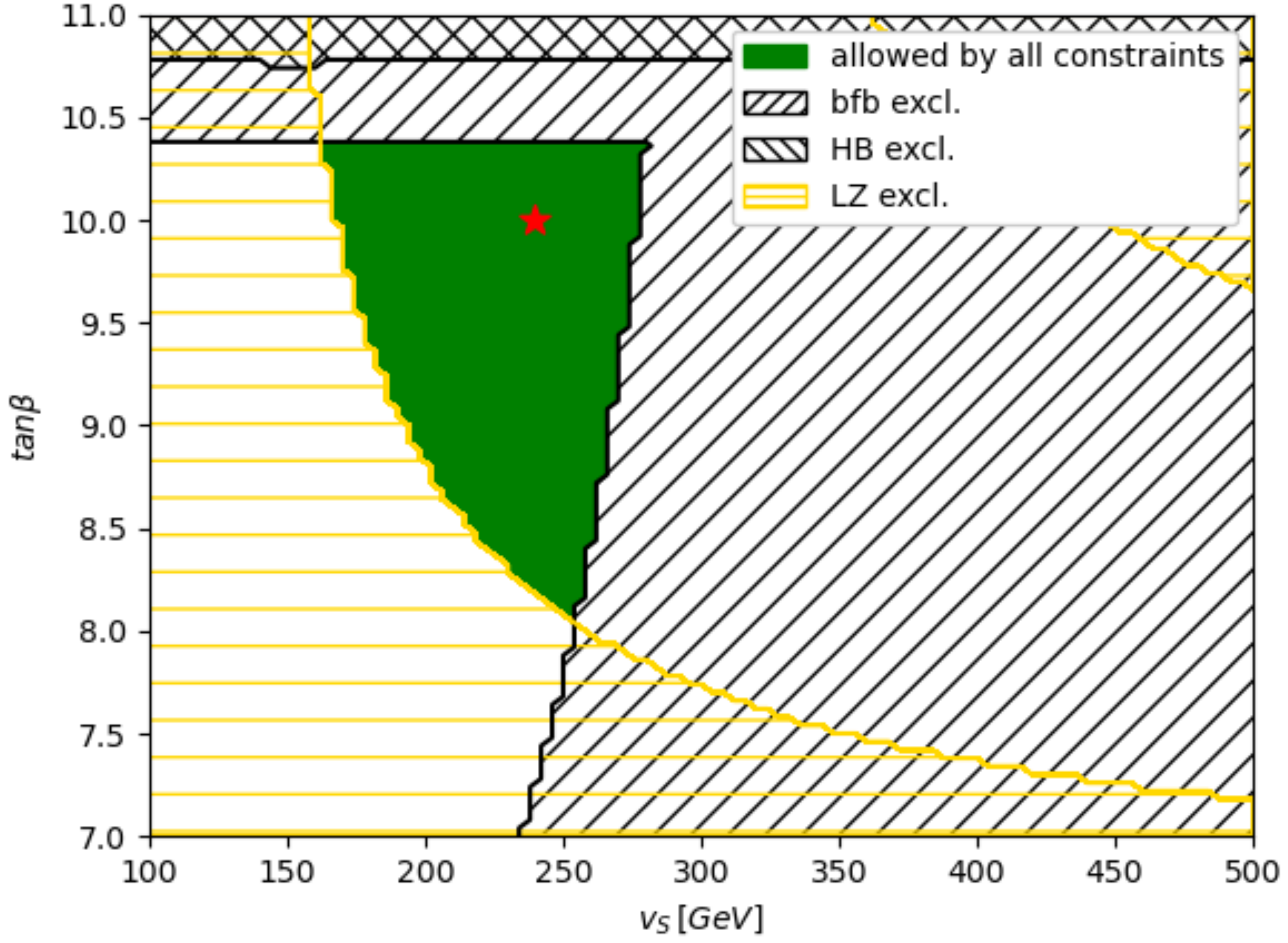

Allowed plane for tan $\beta - v_S$

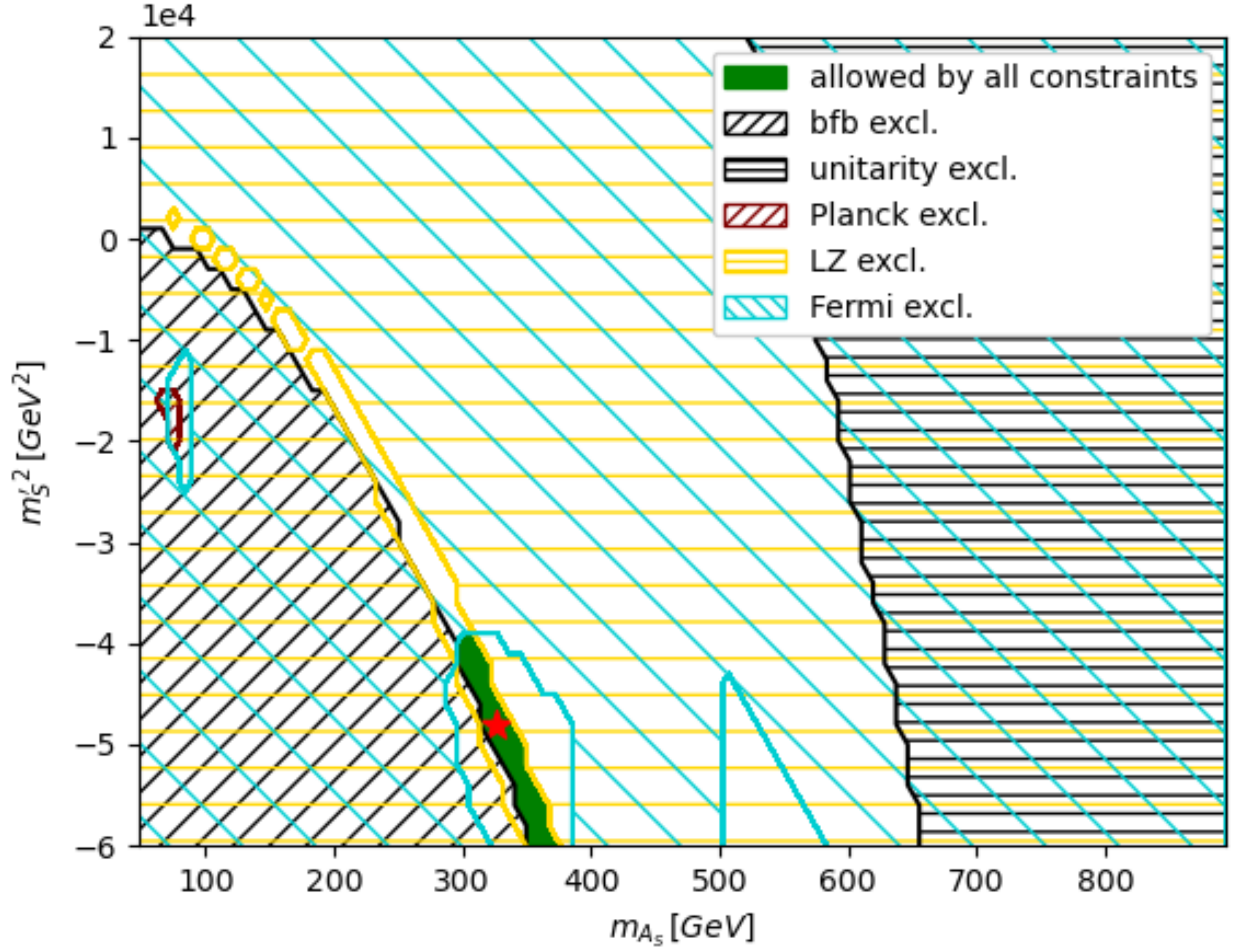

Allowed plane for $m_S^{2\prime} - m_{A_S}$

Salient Features: $m_S^{2\prime} - m_{A_S}$ variation

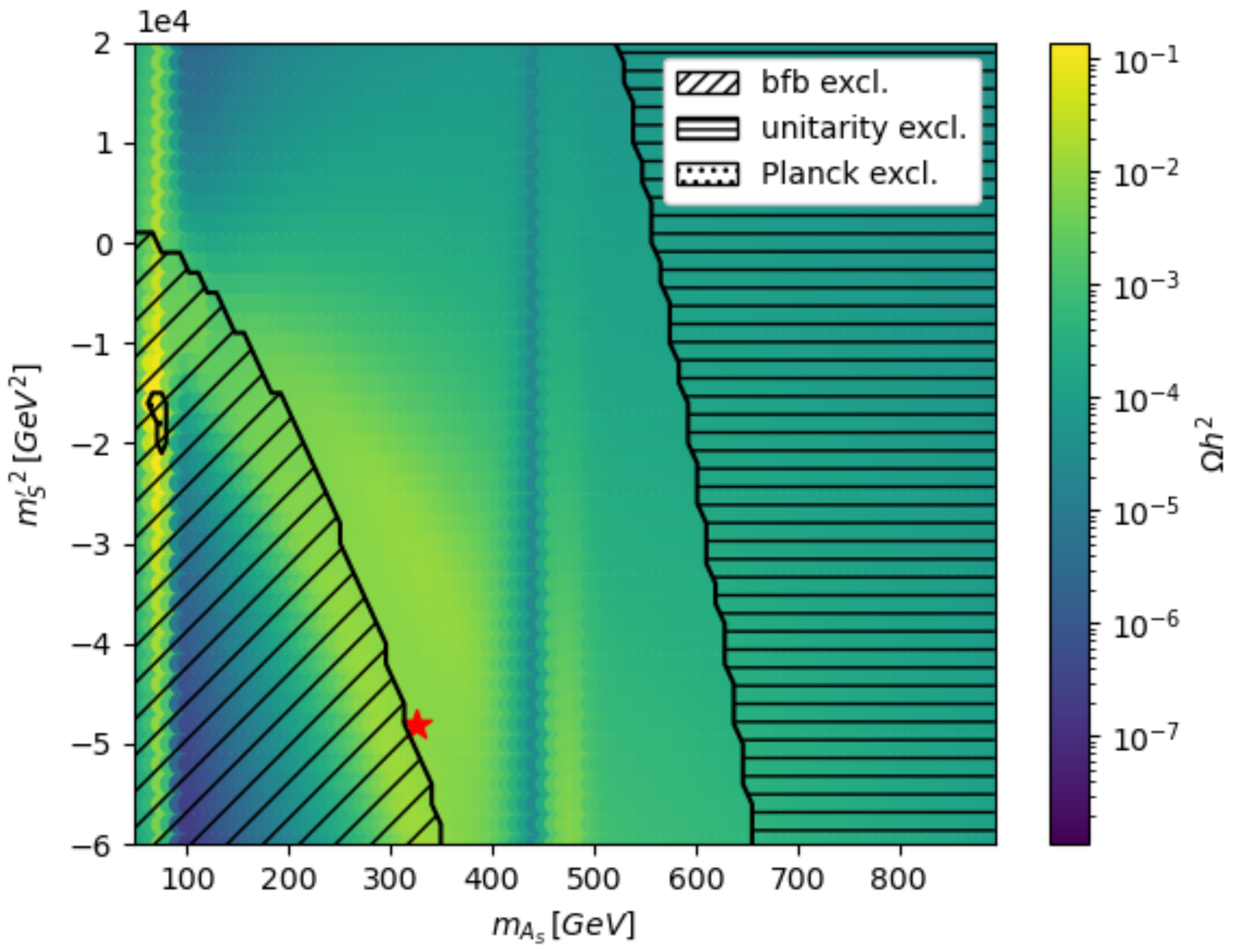

Effect of Relic density constraints.

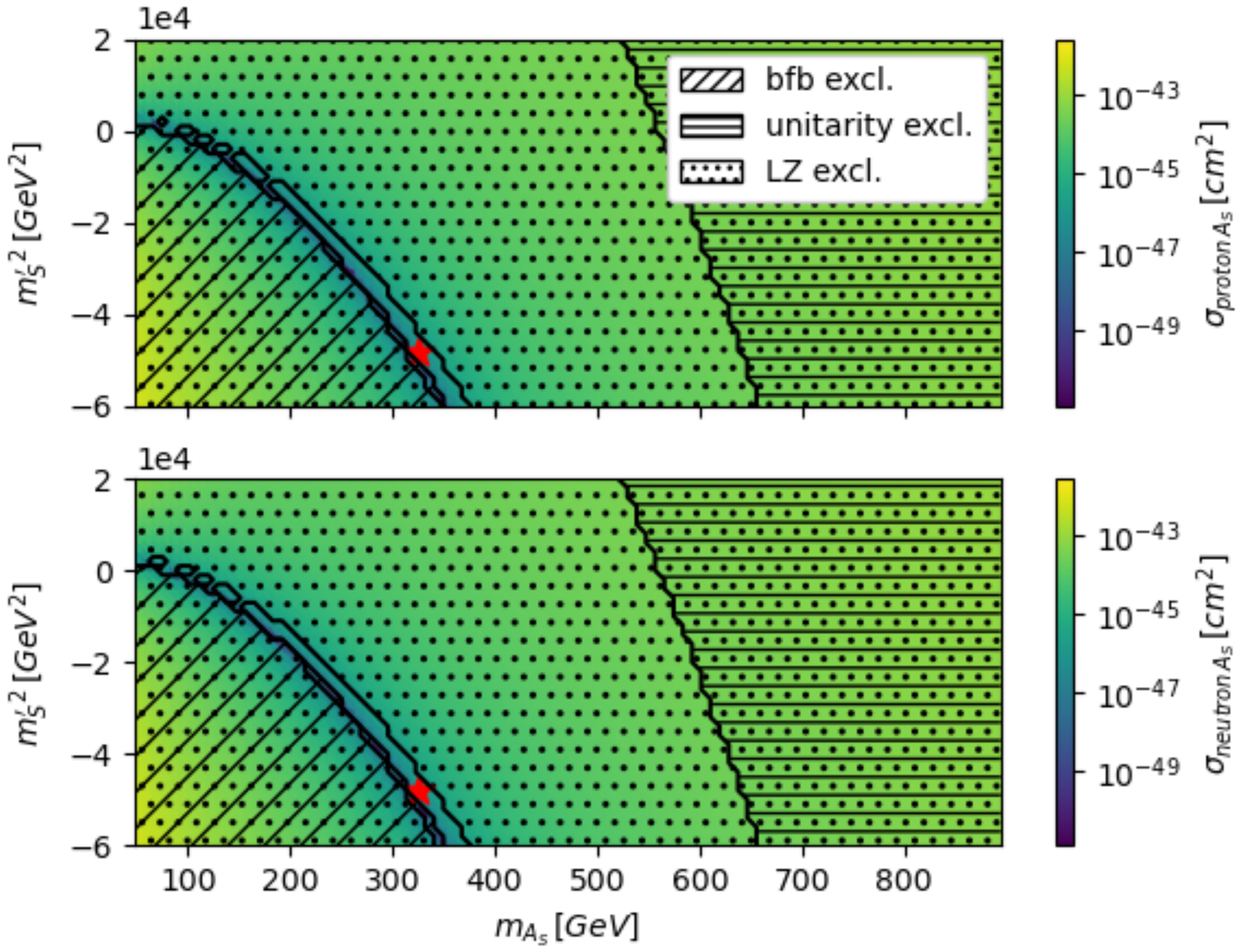

Effect of LZ constraints.

- Dips observed at $m_{A_S} \sim 62, 450$ GeV corresponding to SM Higgs and heavy Higgs resonant regions.
- LZ stringently rules out much of the parameter space for $m_S^{2\prime} - m_{A_S}$ plane.

Backgrounds

Preliminary results.

Process	Production cross-section (pb) at $\sqrt{s} =$	
	1 TeV	3 TeV
$\gamma\nu\bar{\nu}$	2.447	2.964

Whizard cross sections for SM background at $\sqrt{s} = 1$ and 3 TeV.

Benchmark	Production cross-section		
	at $\sqrt{s} = 250$ TeV	at $\sqrt{s} = 500$ GeV	at $\sqrt{s} = 1$ TeV
BP55	4.42 fb	1.1 fb	0.24 fb
$\nu\nu Z$ background	503 fb	491 fb	950 fb

Mono-Z cross-sections for BP55 and for SM background.

The SM Lagrangian

$$\mathcal{L}_{SM} = \mathcal{L}_f + \mathcal{L}_G + \mathcal{L}_H + \mathcal{L}_Y$$

$$\mathcal{L}_f = \bar{q}_L i \not{D} q_L + \bar{u}_R i \not{D} u_R + \bar{d}_R i \not{D} d_R + \bar{\ell}_L i \not{D} \ell_L + \bar{e}_R i \not{D} e_R \qquad D_\mu = \partial_\mu + i g' \frac{Y}{2} B_\mu + i g \frac{\vec{\sigma}}{2} . \vec{W}_\mu + i \frac{g_s}{2} \lambda_a G^a_\mu$$

- $$\mathcal{L}_G = -\frac{1}{4} G^{a\mu\nu} G_{a\mu\nu} - \frac{1}{4} B^{\mu\nu} B_{\mu\nu} - \frac{1}{4} W^{k\mu\nu} W^k_{\mu\nu} \qquad G^a_{\mu\nu} = \partial_\mu G^a_\nu - \partial_\nu G^a_\mu - g_s f^{abc} G^b_\mu G^c_\nu$$

$$B_{\mu\nu} = \partial_\mu B_\nu - \partial_\nu B_\mu,$$

$$W^k_{\mu\nu} = \partial_\mu W^k_\nu - \partial_\nu W^k_\mu - g \epsilon^{ijk} W^i_\mu W^j_\nu$$

- $$\mathcal{L}_H = |D_\mu \phi|^2 + \mu^2 \phi^\dagger \phi - \lambda (\phi^\dagger \phi)^2$$

- $$\mathcal{L}_Y = -y^{ij}_u \bar{Q}_i . \phi^c u_{R_j} - y^{ij}_d \bar{Q}_i . \phi \, d_{R_j} - y^{ij}_l \bar{L}_i . \phi \, e_{R_j} + h.c.$$

Spontaneous Symmetry Breaking

Higgs Lagrangian

$$\mathcal{L}_H = |D_\mu \phi|^2 - V_H$$

Scalar potential

$$V_H = -\mu^2 \phi^\dagger \phi + \lambda(\phi^\dagger \phi)^2 \, . \quad \phi = \begin{pmatrix} \phi^+ \\ \phi^0 \end{pmatrix}$$

$$\phi = \frac{1}{\sqrt{2}} \begin{pmatrix} \phi_1 + i\phi_2 \\ \phi_3 + i\phi_4 \end{pmatrix}$$

For $\mu^2 > 0$,

$$\frac{v}{\sqrt{2}} = \frac{\sqrt{\mu^2}}{2\lambda}$$

where $\phi^\dagger \phi = \frac{v^2}{2}$. Writing ϕ in the unitary gauge as

$$\phi = \frac{1}{\sqrt{2}} \begin{pmatrix} 0 \\ v + h \end{pmatrix}$$

$$\boxed{m_f = y_f \frac{v}{\sqrt{2}}} \qquad \boxed{m_h = v\sqrt{2\lambda} \, .} \qquad \boxed{m_W = \frac{1}{2} g \, v} \qquad \boxed{m_Z = \frac{1}{2}\sqrt{(g^2 + g'^2)} \, v}$$

Minimization Equations

$$
\begin{aligned}
m_{11}^2 v_1 - m_{12}^2 v_2 + \frac{\lambda_1}{2} v_1^3 + \frac{\lambda_{345}}{2} v_1 v_2^2 + (\frac{\lambda_1'}{2} v_1 + \lambda_4' v_1) v_S^2 &= 0, \\
m_{22}^2 v_2 - m_{12}^2 v_1 + \frac{\lambda_2}{2} v_2^3 + \frac{\lambda_{345}}{2} v_1^2 v_2 + (\frac{\lambda_2'}{2} v_2 + \lambda_5' v_2) v_S^2 &= 0, \\
m_S^2 v_S + m_S'^2 v_S + \frac{\lambda_1''}{12} v_S^3 + \frac{\lambda_2''}{3} v_S^3 + \frac{\lambda_3''}{4} v_S^3 + \frac{v_S}{2} (\lambda_1' v_1^2 + \lambda_2' v_2^2) + & \\
v_S (\lambda_4' v_1^2 + \lambda_5' v_2^2) &= 0.
\end{aligned}
$$

Scalar Mass Matrix

$$M_S^2 = \begin{pmatrix} m_{12}^2 \frac{v_2}{v_1} + \lambda_1 v_1^2 & -m_{12}^2 + \lambda_{345} v_1 v_2 & (\lambda_1' + 2\lambda_4') v_1 v_S \\ -m_{12}^2 + \lambda_{345} v_1 v_2 & m_{12}^2 \frac{v_1}{v_2} + \lambda_2 v_2^2 & (\lambda_2' + 2\lambda_5') v_2 v_S \\ (\lambda_1' + 2\lambda_4') v_1 v_S & (\lambda_2' + 2\lambda_5') v_2 v_S & (\frac{5\lambda_1''}{6} + \frac{\lambda_3''}{2}) v_S^2 \end{pmatrix}$$

Basis change

$$R = \begin{pmatrix} c_{\alpha_1} c_{\alpha_2} & s_{\alpha_1} c_{\alpha_2} & s_{\alpha_2} \\ -s_{\alpha_1} c_{\alpha_3} - c_{\alpha_1} s_{\alpha_2} s_{\alpha_3} & c_{\alpha_1} c_{\alpha_3} - s_{\alpha_1} s_{\alpha_2} s_{\alpha_3} & c_{\alpha_2} s_{\alpha_3} \\ s_{\alpha_1} s_{\alpha_3} - c_{\alpha_1} s_{\alpha_2} c_{\alpha_3} & -c_{\alpha_1} s_{\alpha_3} - s_{\alpha_1} s_{\alpha_2} c_{\alpha_3} & c_{\alpha_2} c_{\alpha_3} \end{pmatrix}$$

$$\begin{aligned}
\lambda_1 &= \frac{1}{v^2 \cos^2\beta}(\Sigma_{i=1}^3 m_i^2 R_{i1}^2 - \tilde{\mu}^2 \sin^2\beta), \\
\lambda_2 &= \frac{1}{v^2 \sin^2\beta}(\Sigma_{i=1}^3 m_i^2 R_{i2}^2 - \tilde{\mu}^2 \cos^2\beta), \\
\lambda_3 &= \frac{1}{v^2}\left(\frac{1}{\sin\beta\cos\beta}\Sigma_{i=1}^3 m_i^2 R_{i1} R_{i2} - \tilde{\mu}^2 + 2m_{H^\pm}^2\right), \\
\lambda_4 &= \frac{1}{v^2}(m_A^2 + \tilde{\mu}^2 - 2m_{H^\pm}^2), \\
\lambda_5 &= \frac{1}{v^2}(-m_A^2 + \tilde{\mu}^2), \\
\lambda_1' &= \frac{1}{3}\left(\frac{1}{v v_S \cos\beta}\Sigma_{i=1}^3 m_i^2 R_{i1} R_{i3} - 2\delta_{14}'\right), \\
\lambda_2' &= \frac{1}{3}\left(\frac{1}{v v_S \sin\beta}\Sigma_{i=1}^3 m_i^2 R_{i2} R_{i3} - 2\delta_{25}'\right), \\
\lambda_4' &= \frac{1}{3}\left(\frac{1}{v v_S \cos\beta}\Sigma_{i=1}^3 m_i^2 R_{i1} R_{i3} + \delta_{14}'\right), \\
\lambda_5' &= \frac{1}{3}\left(\frac{1}{v v_S \sin\beta}\Sigma_{i=1}^3 m_i^2 R_{i2} R_{i3} + \delta_{25}'\right), \\
\lambda_1'' &= \lambda_2'' = -\frac{3}{2v_S^2} \\
&\quad \times \left(2m_S^{2\prime} + 2v^2\left(\frac{1}{3}(\frac{1}{v v_S \cos\beta}\Sigma_{i=1}^3 m_i^2 R_{i1} R_{i3} + \delta_{14}')\cos^2\beta\right.\right. \\
&\quad \left.\left. + \frac{1}{3}\left(\frac{1}{v v_S \sin\beta}\Sigma_{i=1}^3 m_i^2 R_{i2} R_{i3} + \delta_{25}'\right)\sin^2\beta\right) + m_{A_S}^2\right), \\
\lambda_3'' &= \frac{1}{3}\left(\frac{6}{v_S^2}\Sigma_{i=1}^3 m_i^2 R_{i3}^2\right. \\
&\quad + \frac{15}{2v_S^2}\left(2m_S^{2\prime} + 2v^2\left(\frac{1}{3}\left(\frac{1}{v v_S \cos\beta}\Sigma_{i=1}^3 m_i^2 R_{i1} R_{i3} + \delta_{14}'\right)\cos^2\beta\right.\right. \\
&\quad \left.\left.\left. + \frac{1}{3}\left(\frac{1}{v v_S \sin\beta}\Sigma_{i=1}^3 m_i^2 R_{i2} R_{i3} + \delta_{25}'\right)\sin^2\beta\right) + m_{A_S}^2\right)\right), \\
m_{12}^2 &= \tilde{\mu}^2 \cdot \sin\beta\cos\beta, \qquad (2.15)
\end{aligned}$$

DM couplings

$$
\begin{aligned}
\frac{\lambda_{h_j A_S A_S}}{v} &= -[(\lambda_1' - 2\lambda_4')c_\beta R_{j1} + (\lambda_2' - 2\lambda_5')s_\beta R_{j2} - \frac{v_S}{2v}(\lambda_1'' - \lambda_3'')R_{j3}], \\
\lambda_{h_j h_k A_S A_S} &= -[(\lambda_1' - 2\lambda_4')R_{j1}R_{k1} + (\lambda_2' - 2\lambda_5')R_{j2}R_{k2} - \frac{1}{2}(\lambda_1'' - \lambda_3'')R_{j3}R_{k3}],
\end{aligned}
$$

BFB

in the basis $X = \left(\Phi_1^\dagger\Phi_1,\ \Phi_2^\dagger\Phi_2,\ \rho_S^2,\ \eta_S^2\right)^T$, with $S = \rho_S + i\eta_S$:

$$
\begin{aligned}
min[V_4] &= X^T \frac{1}{2} \underbrace{\begin{pmatrix} \lambda_1 & \lambda_3 + \rho^2(\lambda_4 - |\lambda_5|) & \lambda_1' + 2\lambda_4' & \lambda_1' - 2\lambda_4' \\ \lambda_3 + \rho^2(\lambda_4 - |\lambda_5|) & \lambda_2 & \lambda_2' + 2\lambda_5' & \lambda_2' - 2\lambda_5' \\ \lambda_1' + 2\lambda_4' & \lambda_2' + 2\lambda_5' & \frac{5\lambda_1''+3\lambda_3''}{6} & \frac{-\lambda_1''+\lambda_3''}{2} \\ \lambda_1' - 2\lambda_4' & \lambda_2' - 2\lambda_5' & \frac{-\lambda_1''+\lambda_3''}{2} & \frac{-\lambda_1''+\lambda_3''}{2} \end{pmatrix}}_{A} X \\
&= \frac{1}{2} X^T A X,
\end{aligned}
\tag{3.1}
$$

where two cases are distinguished:

$$
\begin{aligned}
&\text{case 1: } (\lambda_4 - |\lambda_5|) \geq 0 \quad \Rightarrow \quad \min[V_4] = V_4|_{\rho=0} \\
&\text{case 2: } (\lambda_4 - |\lambda_5|) < 0 \quad \Rightarrow \quad \min[V_4] = V_4|_{\rho=1}.
\end{aligned}
$$

The explicit copositivity conditions for a symmetric order 3 matrix B with entries b_{ij}, $i, j = 1, 2, 3$ can be found in [53, eq. (5) and (6)] and are:

$$b_{11} \geq 0, \quad b_{22} \geq 0, \quad b_{33} \geq 0, \tag{3.2}$$

$$\bar{b_{12}} = b_{12} + \sqrt{b_{11}b_{22}} \geq 0, \tag{3.3}$$

$$\bar{b_{13}} = b_{13} + \sqrt{b_{11}b_{33}} \geq 0, \tag{3.4}$$

$$\bar{b_{23}} = b_{23} + \sqrt{b_{22}b_{33}} \geq 0, \tag{3.5}$$

$$\sqrt{b_{11}b_{22}b_{33}} + b_{12}\sqrt{b_{33}} + b_{13}\sqrt{b_{22}} + b_{23}\sqrt{b_{11}} + \sqrt{2\bar{b_{12}}\bar{b_{13}}\bar{b_{23}}} \geq 0. \tag{3.6}$$

The matrix A has to satisfy: $\det(A) \geq 0 \quad \vee \quad (\mathrm{adj}A)_{ij} < 0$, for some i, j. The adjugate of A is defined as the transpose of the cofactor matrix: $(\mathrm{adj}A)_{ij} = (-1)^{i+j} D_{ji}$, with D_{ij} being the determinant of the submatrix that is obtained by deleting the i-th row and j-th column from A.

95 GeV signal strengths

$$\mu_{\text{LEP}}^{b\bar{b}} = 0.117^{+0.057}_{-0.057}, \qquad \mu_{\text{LHC-combined}}^{\gamma\gamma} = 0.24^{+0.09}_{-0.08},$$

$$\mu_{\text{LEP}}^{\text{the}} = \frac{\sigma_{\text{2HDMS}}(e^+e^- \to Zh_1)}{\sigma_{\text{SM}}(e^+e^- \to ZH^0_{\text{SM}})} \times \frac{\text{BR}_{\text{2HDMS}}(h_1 \to b\bar{b})}{\text{BR}_{\text{SM}}(H^0_{\text{SM}} \to b\bar{b})} = |c_{h_1VV}|^2 \frac{\text{BR}_{\text{2HDMS}}(h_1 \to b\bar{b})}{\text{BR}_{\text{SM}}(H^0_{\text{SM}} \to b\bar{b})}$$

$$\mu_{\text{CMS}}^{\text{the}} = \frac{\sigma_{\text{2HDMS}}(gg \to h_1)}{\sigma_{\text{SM}}(gg \to H^0_{\text{SM}})} \times \frac{\text{BR}_{\text{2HDMS}}(h_1 \to \gamma\gamma)}{\text{BR}_{\text{SM}}(H^0_{\text{SM}} \to \gamma\gamma)} = |c_{h_1tt}|^2 \frac{\text{BR}_{\text{2HDMS}}(h_1 \to \gamma\gamma)}{\text{BR}_{\text{SM}}(H^0_{\text{SM}} \to \gamma\gamma)}$$

$$\chi^2_{\text{CMS-LEP}} = \left(\frac{\mu_{\text{LEP}}^{\text{the}} - 0.117}{0.057}\right)^2 + \left(\frac{\mu_{\text{CMS}}^{\text{the}} - 0.6}{0.2}\right)^2$$

$$c_{h_1tt} = \frac{\sin\alpha_1 \cos\alpha_2}{\sin\beta}, \qquad c_{h_1bb} = \frac{\cos\alpha_1 \cos\alpha_2}{\cos\beta}, \qquad c_{h_1VV} = \cos\alpha_2 \cos(\beta - \alpha_1)\ .$$

S.Heinemeyer et.al,
Phys. Rev. D 106 (2022), no. 7 075003

Couplings in 2HDM

The reduced Higgs to fermion couplings for all four Yukawa types are summarized in Tab. 1.

	type I	type II	lepton-specific	flipped
$c_{h_i tt}$	$\frac{R_{i2}}{\sin\beta}$	$\frac{R_{i2}}{\sin\beta}$	$\frac{R_{i2}}{\sin\beta}$	$\frac{R_{i2}}{\sin\beta}$
$c_{h_i bb}$	$\frac{R_{i2}}{\sin\beta}$	$\frac{R_{i1}}{\cos\beta}$	$\frac{R_{i2}}{\sin\beta}$	$\frac{R_{i1}}{\cos\beta}$
$c_{h_i \tau\tau}$	$\frac{R_{i2}}{\sin\beta}$	$\frac{R_{i1}}{\cos\beta}$	$\frac{R_{i1}}{\cos\beta}$	$\frac{R_{i2}}{\sin\beta}$

Table 1: Higgs to fermion reduced couplings for different type of Yukawa couplings

$$c_{h_i VV} = c_{h_i ZZ} = c_{h_i WW} = \cos\beta R_{i1} + \sin\beta R_{i2}$$

Gauge couplings in 2HDM

S.Heinemeyer et.al,
Phys. Rev. D 106 (2022), no. 7 075003

Scan parameter choices

$$\tan\beta = 10,\ \frac{\tan\beta}{\tan\alpha_1} = 0.35,\ \alpha_2 = -1.2,\ \beta - \alpha_1 - \alpha_3 = -[1.54, 1.6],\ m_{h_1} = 95\ \text{GeV},$$

$$m_{h_2} = 125\ \text{GeV},\ m_{H^\pm} = m_A = m_{h_3} = 900\ \text{GeV},\ v_s = [100, 1000]\ \text{GeV},$$
$$m_{A_s} = [48, 800]\ \text{GeV},\ m_S^{2\prime} = [0, 10^6]\ \text{GeV}^2,\ \lambda_4' = [-3:3],\ \lambda_5' = [-3:3].$$

Significance

$$\mathcal{S} = \sqrt{2[(S+B)\mathrm{Log}(1+\frac{S}{B}) - S]}$$

- SM Background for gluon fusion: 7.07 pb
- SM Background for VBF: 1.12 pb.

Dey et.al JHEP 09 (2019) 004